CHEMICAL EQUILIBRIUM STUDIES OF VANADIUM(V) COMPLEXES AND THEIR EFFECTS ON THE CATALYTIC ACTIVITY OF RIBONUCLEASE A

by

Chui H. Leon-Lai

B.Sc. (Honors), Universidad Santa Maria, Venezuela, 1986

THESIS SUBMITTED IN PARTIAL FULFILLMENT OF
THE REQUIREMENTS FOR THE DEGREE OF
MASTER OF SCIENCE

in the Department
of
Chemistry

SIMON FRASER UNIVERSITY

November 1990

Approval

Name: Chui H. Leon-Lai

Degree: Master of Science

Title of thesis: Chemical equilibrium studies of vanadium(V) complexes and their effects on the catalytic activity of ribonuclease A

Examining Committee:

Chair: Dr. P. Percival

Dr. A. S. Tracey
Senior Supervisor

Dr. W. R. Richards
Associate Professor

Dr. T. J. Borgford
Assistant Professor

Dr. M. J. Gresser
Adjunct Professor

Dr. B. M. Pinto
Internal Examiner
Department of Chemistry
Simon Fraser University

PARTIAL COPYRIGHT LICENSE

I hereby grant to Simon Fraser University the right to lend my thesis, project or extended essay (the title of which is shown below) to users of the Simon Fraser University Library, and to make partial or single copies only for such users or in response to a request from the library of any other university, or other educational institution, on its own behalf or for one of its users. I further agree that permission for multiple copying of this work for scholarly purposes may be granted by me or the Dean of Graduate Studies. It is understood that copying or publication of this work for financial gain shall not be allowed without my written permission.

Title of Thesis/Project/Extended Essay

Chemical Equilibrium Studies of Vanadium(V) Complexes and their Effects on the Catalytic Activity of Ribonuclease A

Author:

(signature)

Chui H. Leon-Lai

(name)

December 7th, 1990

(date)

Abstract

Vanadium nuclear magnetic resonance (^{51}V NMR) spectroscopy and enzyme kinetics were used to study the interactions of inorganic vanadate (V_i) and vanadium(V) complexes with bovine pancreatic ribonuclease A (RNase A) (EC 3.1.27.5). Inorganic vanadate forms complexes with uridine, 5,6-dihydrouridine and methyl β-D-ribofuranoside. By analyzing the ^{51}V NMR and UV spectra of solutions containing V_i and various concentrations of the organic ligands, the stoichiometries and formation constants of the complexes were determined. From the kinetic studies, it was found that the inorganic vanadate and the methyl β-D-ribofuranoside-vanadate complex did not inhibit the RNase A catalyzed hydrolysis of uridine 2',3'-cyclic monophosphate and that the 5,6-dihydrouridine-vanadate complex caused less inhibition than did the uridine-vanadate complex. These results were consistent with the NMR studies, which showed that the inorganic vanadate and methyl β-D-ribofuranoside did not bind to the enzyme while the 5,6-dihydrouridine-vanadate complex bound less tightly than did the uridine-vanadate complex. The inhibition constants (K_i's) of these vanadium(V) complexes were determined in the above studies and the results were consistent with binding at the active site of the enzyme. Approximate K_i values were 2.5×10^{-7} M and 1.4×10^{-6} M for the uridine- and 5,6-dihydrouridine-vanadate complexes, respectively. From pH variation studies, it was found that H^+ is

incorporated into the enzyme/uridine/vanadate complex. The results were interpreted in terms of an induced fit mechanism in which the pyrimidine subsite of the active site must be occupied for the enzyme to be able to bind the transition state or transition state analog tightly.

Dedication

To my parents for their love
and encouragement to achieve
my goals.

Acknowledgments

I would like to thank Dr. Michael J. Gresser and Dr. Alan S. Tracey for their guidance which made possible the writing of this thesis, and their assistance during the experimental work period. Also, I would like to thank Mrs. Marcelline Tracey for her expertise in obtaining NMR spectra plots, and Dr. Paul J. Stankiewicz for his helpful discussions about enzyme kinetics. Thanks is also extended to Mandy Kao, who showed me the use of several instruments, besides her friendship; Marcia Craig, Susana Liu and Philip Chang for their friendship and support; and my brother Ramon for his encouragement.

Table of Contents

List of Tables

List of Figures

List of Abbreviations

A_{270} = absorbance at 270 nm

H_2-U = 5,6-dihydrouridine

HVO_4^{2-} = dianionic monovanadate

$H_2VO_4^-$ = monoanionic monovanadate

H_3PO_4 = phosphoric acid

H_3VO_4 = vanadic acid

I = nuclear spin angular momentum

KHz = kilohertz

K_i = inhibition constant

K_m = Michaelis constant

Me-R = methyl β-D-ribofuranoside

MHz = megahertz

MW = molecular weight

NaH_2VO_4 = monosodium vanadate

NMR = nuclear magnetic resonance

O(3)-2'-CMP = cytidine-N(3)-oxide 2' phosphate

RNA = ribonucleic acid

RNase A = ribonuclease A

U = uridine

U-2',3'-P = uridine 2',3'-cyclic monophosphate

UV = ultraviolet

V_2 = dimeric vanadate

V_4 = tetrameric vanadate

V_2L_2 = binuclear vanadate-ligand (2:2) complex

V_2O_5 = vanadium pentoxide

V(V)-H_2O_2 = vanadium(V)-hydrogen peroxide complex

V_i = inorganic vanadate

VL = mononuclear vanadate-ligand (1:1) complex

Chapter I
Introduction

Vanadium is a widely dispersed element which, in air-saturated aqueous solution above pH 6 is stable in the +5 oxidation state. Vanadium(V) exists as monomeric inorganic vanadate (V_i), and a variety of oligomers in various protonated states (1). When alcohols are present, vanadate spontaneously forms acyclic mono- and diesters (2), while with vicinal diols, it forms both cyclic and acyclic complexes (3-5).

Since the discovery of two vanadium dependent enzymes (a nitrogenase from special strains of *Azotobacter* (6) and a non-heme haloperoxidase from *Ascorphyllum nodosum* (7), vanadium has clearly attained the status of a metal essential at least to certain groups of primitive organisms. Vanadium in trace quantities is also present, although perhaps not essential, in more advanced life forms (rats, chicks), yet toxic in larger amounts (8). Vanadium has a large effect on the action of enzymes, either activating or inhibiting them. Inhibition of ribonuclease by vanadium was the first reported example of the influence of this metal on the activity of an enzyme (9). Vanadate can act as a competitive inhibitor of phosphate and, hence, regulate the effects of both inorganic phosphate and phosphorylated substrates. This activity may derive from its ability to mimic the function of phosphate (10) and to act as a transition-

state analogue. Activation of enzymes seems to occur because vanadate acts as a phosphate analog. Spontaneously formed vanadium esters are accepted as enzyme substrates instead of the normally phosphorylated substrates. This activation has been demonstrated in enzymes which do not catalyze cleavage of a bond to the phosphorus atom (11). The first report of a vanadate ester acting as a substrate analog is the ester, glucose-6-vanadate, which can be utilized by glucose-6-phosphate dehydrogenase to catalyze the formation of gluconic acid (10). Another example is the ester, glycerol-3-vanadate, which is accepted by glycerol-3-phosphate dehydrogenase in catalysing the formation of dihydroxyacetone (12, Craig & Gresser unpub.). There is also evidence that phosphoglucose isomerase, phosphoribose isomerase, ribulose-5-phosphate epimerase and adenylate kinase accept vanadate esters as substrate analogs (11,13).

Vanadium is known to inhibit many enzymes which catalyze phosphoryl transfer reactions, where cleavage of P-O bonds is involved (11). The inhibition is caused mainly, but not exclusively, by vanadate (vanadium(V)). The similarity between the chemistry of vanadate and phosphate is the major cause for the biological activity of vanadate. Bond lengths and pK_a's are very similar in both ions: V-O bond lengths are around 0.17 nm compared to P-O bond lengths which are around 0.152 nm; vanadic acid (H_3VO_4) possesses pK_a's of 3.5, 7.8 and 12.5 and phosphoric acid (H_3PO_4) possesses pK_a's of 1.7,

6.5 and 12.1 (1). When ligands such as diols are present, vanadate can readily form a vanadate-ligand complex with a trigonal bipyramidal geometry. There is evidence that the transition state of phosphate in enzyme catalyzed phosphoryl transfer reactions has this same geometry (14), so the vanadate-ligand complex would be a transition state analog. Since the vanadium of these vanadate complexes when in solution can readily adopt a trigonal bipyramidal geometry, while phosphate compounds (in this case, nucleotides) cannot readily do so, the K_i of the vanadate complex is much smaller than the K_m of the substrate. The stability of pentacoordinate vanadate complexes, relative to pentacoordinate phosphate species can be explained in the following terms: The valence electron orbitals of the vanadium atom are 3d and 4s, while those of the phosphorus atom are 3s and 3p. When the electron pair of the incoming ligand is accepted by an orbital of the central atom, the energy gap between the highest energy level valence orbital and the lowest energy level unoccupied orbital is much smaller for vanadium than for phosphorus. The 3d orbitals of phosphorus have a relatively much higher energy level than the 3d and 4p orbitals of vanadium (15). As mentioned earlier, since the vanadate-ligand complex exists as a very stable pentacoordinate species in solution, a strong binding or inhibition of some enzymes which catalyze phosphoryl transfer reactions might be predicted. The enzyme-vanadate-ligand complex lies in a depression on the potential energy curve. The deeper the

depression, the longer the lifetime of the complex. If this is the case, this vanadate-ligand complex is a very good transition state analog. In the case of the phosphate-ligand complex, this complex exists mainly as a tetrahedral species in solution. Since the transition state of these reactions is believed to be a pentacoordinate phosphorus, energy is required to overcome the barrier to reach the transition state, i.e., the high activation energy of the enzyme-phosphate-ligand complex transition state implies that the step from reactants to transition state is a very energetically demanding reaction. Tight binding of the transition state by the enzyme decreases the activation energy, and is responsible for catalysis of the reaction by the enzyme. This is why transition state analogs are potent inhibitors. Examples of strong inhibition by vanadate complexes can be seen in phosphoglucomutase (16), phosphoglycerate mutase (17), and ribonuclease (9); but no significant inhibition by vanadate itself can be detected.

In general, depending on the effect exerted by vanadates on phosphoryl transfer enzymes, these can be classified in the following way: a) Enzymes which catalyze the transfer of phosphate from a phosphorylated enzyme intermediate to water, b) enzymes which do not catalyze reactions of nucleoside 5'-phosphates, c) enzymes which catalyze reactions of nucleoside 5'-phosphates. Enzymes of group a) are inhibited by vanadate and its complexes, enzymes of group b) are not inhibited by vanadate alone but by its

complexes, and enzymes of group c) are not strongly inhibited either by vanadate or its complexes, with some exceptions (11).

Vanadium may be utilized as a tool in bioresearch. The suppressant effect of vanadium(IV) ribonucleoside complexes on ribonuclease activity of cell homogenates has been very useful in isolating intact mRNA from lymphocytes (18). Vanadate complexes are also useful as mechanistic probes (11), since it has been shown that the inhibition of some phosphoryl transfer enzymes is quite selective. It is also possible that vanadium may prove to be useful as a drug for the treatment of various diseases such as diabetes (19-22), and sickle cell anemia (23). There is evidence that vanadium may be involved in glucose metabolism, renal and bladder function, the sodium pump, muscle contractions and other physiological processes (1).

Ribonuclease A is a digestive enzyme secreted by the pancreas. Probably the best-characterized nuclease is bovine pancreatic ribonuclease A, which is an endonuclease (24). It has the ability to bind both pyrimidine and purine nucleotides (24,25).

The amino acid sequence of RNase A has been published elsewhere (24,25). Although a number of crystallographic investigations have elucidated the three-dimensional structure of RNase A (26-28) and its proteolytic modification RNase S (24,29), many details of the mechanism of action of this enzyme still remain to be conclusively determined. X-ray and neutron diffraction studies

have shown that the active site of RNase A (27,28,30) is composed of three ionizable groups which are implicated in the binding mechanism and the catalytic reaction; two of these groups are His-12 and His-119 with approximate pK_a values of 5.8 and 6.2 respectively (31,32), and the remaining amino acid residue is Lys 41 with a pK_a value of 9.0 (33). A partial drawing of the active site is shown in Fig. I.1. The currently accepted mechanism of action (34) involves formation and decomposition of the cyclic 2',3'-nucleotide (an intermediate in the hydrolysis of RNA) by closely similar processes as shown in Fig. I.2 (35).

Competitive inhibitors are especially useful for elucidating the nature of the active site of enzymes, since they act on the site selectively and directly in competition with substrates and coenzymes. Aside from the question of affinity, the most important aspect in the study of an inhibitor concerns its mode of binding. In this sense, vanadium is a very useful probe for the study of RNase A. The outstanding NMR properties of the ^{51}V isotope make NMR a useful technique for the study of vanadium(V)-protein interactions (36), as outlined in section II.1.

The main purpose of this study is to determine the magnitude of the dissociation constant (K_i) of the uridine-vanadate complex from RNase A. This complex is the inhibitory species as determined by crystallographic studies. A K_i value of 1.2×10^{-5} M has been reported (9), however, this value for K_i is underestimated

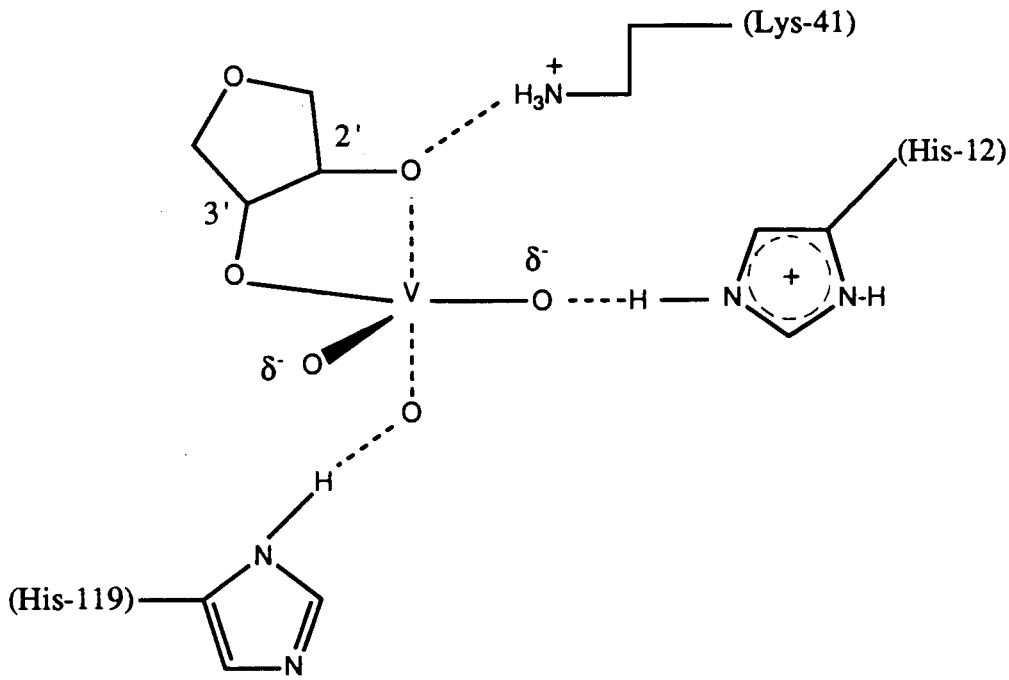

Fig. I.1

Partial structure for the transition state analog of RNase A-catalyzed hydrolysis of U-2',3'-P, according to x-ray and neutron diffraction studies (ref. 25,26,28).

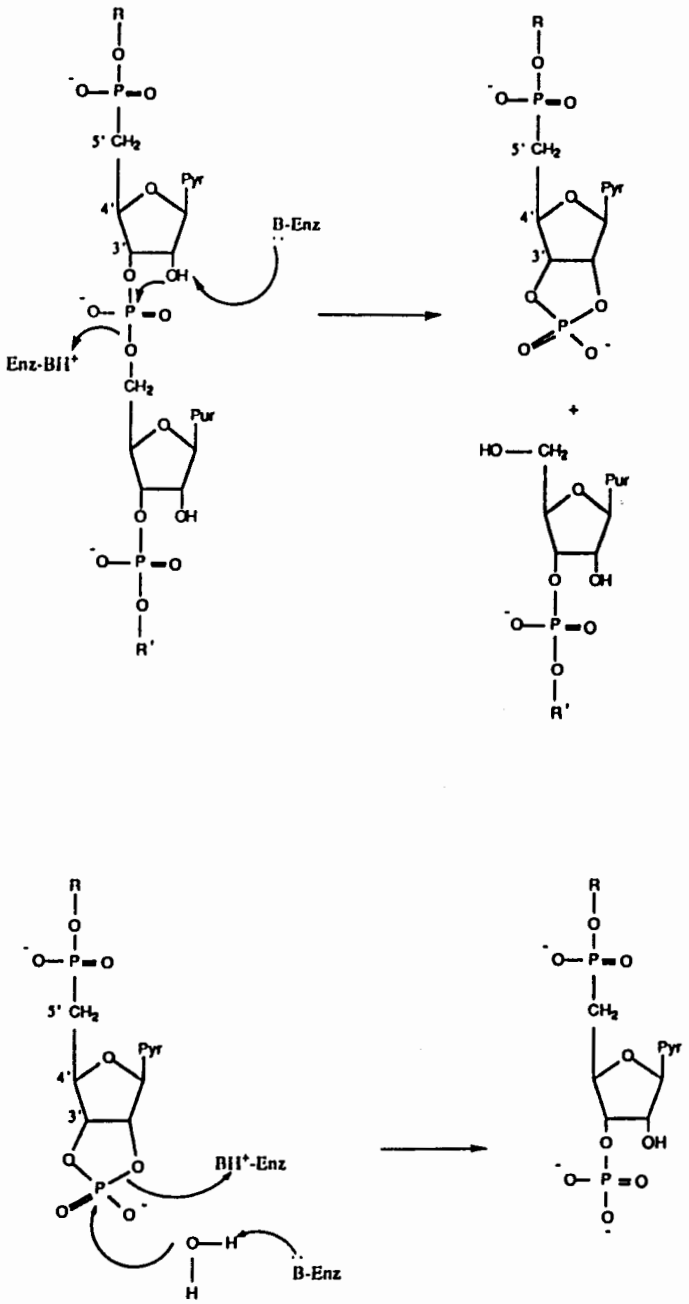

Fig. I.2

Mechanism of hydrolysis of RNA catalyzed by RNase A.

since it has been shown that a binuclear complex of vanadate (a (2:2) uridine-vanadate complex) is the predominant chemical species in solution (5) and that the mononuclear complex is present only in minute quantities. Since the presence of the binuclear complex was not taken into account, the value for the equilibrium constant for formation of the mononuclear complex was overestimated. This means that this complex is a much more potent inhibitor than it had been thought to be. Therefore, a detailed reinvestigation of the magnitude of this inhibition was considered appropriate. ^{51}V NMR spectroscopy and UV absorption spectroscopy of solutions containing vanadate and various concentrations of ribose-containing ligands have been carried out in order to determine the formation constants of these complexes. Also, ^{51}V NMR spectroscopy was used to study directly the binding of these vanadate complexes to RNase A, and the inhibition was investigated by enzyme kinetics. A quantitative comparison of the kinetic parameters characterizing the RNase A-catalyzed hydrolysis of uridine 2',3'-cyclic phosphates in the presence of certain inhibitors is of interest in order to assess the role of the pyrimidine base in the reaction mechanism.

This work describes the inhibition of the enzyme RNase A by complexes that the nucleosides uridine and 5,6-dihydrouridine form with inorganic vanadate.

Chapter II
Chemistry of Vanadium(V) Complexes

II.1. ^{51}V NMR Spectroscopy

Vanadium is 99.76 % abundant as the ^{51}V isotope (I = 7/2) and only 0.24 % corresponds to ^{50}V (I = 6). NMR spectroscopy of ^{51}V metal ion can be very useful since the NMR receptivity of the ^{51}V nucleus is exceptionally high (0.381) due to a large magnetic moment (37). At a resonance frequency of 105 MHz, vanadium(V) signals are relatively well resolved to allow chemical structures to be assigned to all signals. The use of a high-field NMR spectrometer represents an advantage over using a lower field spectrometer since ^{51}V signals tend to be broad due to quadrupolar relaxation. For vanadium(V) species with tetrahedral symmetry, the corresponding signals are relatively sharp (half linewidth = 50-100 Hz) while for species with lower degree of symmetry, the signals may be significantly broader (3).

II.1.1. Experimental procedure

II.1.1.1. Materials

Bovine pancreatic ribonuclease A (lyophilized powder) was purchased from Boehringer Mannheim. All other reagents used were of reagent grade. Enzyme and reagents were used without further purification.

Vanadium(V) oxide, 99.999% (gold label) and 99.99% was purchased from Aldrich Chemical Co.

Uridine 2',3'-cyclic monophosphate (sodium salt), uridine, 5,6-dihydrouridine and methyl β-D-ribofuranoside (crystalline), were purchased from Sigma Chemical Co.

Tris (hydroxymethyl) aminomethane hydrochloride and Tris (hydroxymethyl) aminomethane were purchased from Boehringer Mannheim and Sigma Chemical Co.

KCl was obtained from BDH Chemicals.

HCl (1 N) was obtained from BDH Chemicals.

NaOH (1 N) was obtained from Anachemia Chemicals Inc. and Fisher Scientific.

Reference buffer solutions (pH 4, 7 and 10) were obtained from Canlab.

II.1.1.2. Preparation of vanadate, uridine, 5,6-dihydrouridine and methyl β-D-ribofuranoside stock solutions

Stock solutions of sodium vanadate (NaH_2VO_4) were prepared by dissolving 0.5 mol equiv of vanadium pentoxide (V_2O_5) in 1.0 M NaOH. The mixture was stirred overnight until the orange color of decavanadate disappeared, giving a colorless solution. The solution was diluted with deionized distilled water to give a final concentration of 0.1 M NaH_2VO_4.

Stock solutions of uridine, 5,6-dihydrouridine and methyl β-D-ribofuranoside were prepared by dissolving them in 5.0 mM Tris buffer, and the pH was adjusted to 7.0 with 0.1 N HCl or 0.1 N NaOH. The concentration of Tris buffer was low enough that formation of a significant amount of the vanadate ester could be avoided when preparing the samples.

II.1.1.3. Instrumentation

^{51}V NMR spectra were obtained at 105 MHz on a Bruker WM-400 NMR spectrometer. The acquisition parameters were 0.05-s acquisition times, 50-KHz sweep widths, 50° pulse widths and unlocked mode. Each spectrum was the result of 20,000 scans for vanadate concentrations above 0.1 mM, and 100,000 scans for vanadate concentrations below 0.1 mM. The spectra were zero filled from 4K to 8K and a line broadening factor of 50 Hz was used before transformation to the frequency domain. The Fourier transformation was done in the absolute intensity mode to allow signal intensities from different spectra to be compared. The external reference standard used in this case was $VOCl_3$ whose signal was assigned as 0 ppm, so chemical shifts were reported relative to this standard. In some cases, where the Fourier transformation was done in the relative intensity mode, the external reference used was a complex of V(V)-H_2O_2 whose signals were assigned as -765 ppm and -625 ppm. This chemical shift reference was chosen because its signals do

not interfere with the signals of the vanadate species of interest. Spectra were obtained at room temperature. Baseline correction was performed before measurement of signal intensities. The instrument manufacturer's software was used for all NMR measurements.

II.1.1.4. Equilibrium studies of vanadate in the presence of ligands.

In order to determine the equilibrium constants for formation of the different vanadate complexes, with uridine, 5,6-dihydrouridine and methyl β-D-ribofuranoside, ligand titration experiments were performed. The conditions for these experiments were 5.0 mM Tris, 0.35 M ionic strength with added KCl and 1.0 mM vanadate, pH 7.0. The concentration range used for the ligands was 0-30 mM. The equilibrium constants to be investigated are given in equations 1 and 2 or 1 and 3.

$$V_i + L \overset{K_1}{\rightleftharpoons} VL \qquad [V_i]\,[L]\,K_1 = [VL] \qquad (1)$$

$$2\ VL \overset{K'_2}{\rightleftharpoons} V_2L_2 \qquad [VL]^2\,K'_2 = [V_2L_2] \quad \text{or} \qquad (2)$$

$$2\ V_i + 2\ L \overset{K_3}{\rightleftharpoons} V_2L_2 \qquad [V_i]^2\,[L]^2\,K_3 = [V_2L_2] \qquad (3)$$

II.1.2. Results and discussion: Chemical equilibrium studies of vanadate in the presence of several ligands

The formation of complexes of vanadate with several ligands containing a ribose group have been studied by ^{51}V NMR.

Ligands were uridine, 5,6-dihydrouridine and methyl β-D-ribofuranoside. Although the vanadate-uridine system has previously been studied (5), it was desirable to study this system under the conditions used in this work. The distribution of the signals is shown in Tables II.1-II.3b. The signals arising at -560 ppm, -573 ppm and -576 ppm correspond to free monomeric, dimeric and tetrameric vanadate species. A small amount of tetrahedral vanadate esters is present under the signal arising at -560 ppm, at the higher ligand concentrations. The small resonance at -584 ppm probably corresponds to pentameric vanadate. Signals are relatively sharp due to the symmetry of tetrahedral vanadate.

A new signal arising in the region of -522 to -525 ppm upon addition of ligand is assigned to a vanadate-ligand complex whose geometry is suggested to be trigonal bipyramidal. Since compounds with such a geometry possess a lower degree of symmetry, the signals are expected to be broader. From analysis of these spectra it was determined that the species responsible for this signal is a complex with two ligands and two vanadium atoms.

It is known that vanadate forms cyclic esters with 1,2 diols. In the case of ribose-containing compounds, vanadate esterifies the 2'- and 3'- hydroxyl groups of the ligands to form a cyclic compound analogous to the reacting portion of the RNase A substrate, uridine 2',3'-cyclic monophosphate. The evidence for the formation of this vanadate compound is the appearance of a signal in the region of

-522 to -525 ppm in the ^{51}V NMR spectra of solutions containing an organic ligand (uridine, 5,6-dihydrouridine or methyl β-D-ribofuranoside) and vanadate. This ^{51}V NMR signal is absent in a vanadate solution containing 2',3'-isopropylideneuridine (where the 2'- and 3'-OH groups are blocked) or 2'-deoxyuridine (5), indicating that the 2'- and 3'-OH groups are essential for vanadate complexation. This signal is also absent in a vanadate solution containing 1,3-propanediol (38) suggesting that vanadate does not form a cyclic complex with the 3'- and 5'-OH groups of ribose containing ligands. Further evidence of vanadate esterification of the 2'- and 3'- hydroxyl groups is a 0.5 ppm-chemical shift for $H2'$ and $H3'$ signals in the ^{1}H NMR spectra of a solution containing inosine and vanadate (39). The major species that gives rise to a signal in the region of -522 to -525 ppm is an anhydride containing two pentacoordinate vanadium atoms linked through an oxygen atom with each subunit of the anhydride containing one ligand (V_2L_2). Evidence indicating that the vanadium atom is pentacoordinate comes from a ^{51}V NMR study using vanadate and 1,2-propanediol which is an asymmetric diol (3). Two broader signals than the ones corresponding to tetrahedral vanadate were observed, indicating the asymmetry about the vanadium nucleus. Water stoichiometry studies also indicate that this vanadium is pentacoordinate. A trigonal bipyramidal geometry, was suggested for these cyclic complexes (3). The proposed structures of the vanadate mononuclear

complexes with uridine, 5,6-dihydrouridine and methyl β-D-ribofuranoside are shown in Fig. II.1.

Based on information obtained in previous work (5), equations 1, 2 and the following equilibrium were taken into account in analyzing the results:

$$4\ V_i \underset{}{\overset{K_4}{\rightleftharpoons}} V_4 \qquad [V_i]^4\, K_4 = [V_4] \qquad (4)$$

where V_i = inorganic monovanadate, and V_4 = tetravanadate.

Assuming that the broad signal in the region of -522 to -525 ppm is due to a mixture of (1:1) vanadate-ligand complex (VL) and (2:2) vanadate-ligand complex (V_2L_2), equation 5 is obtained from equations 1 and 2.

$$[VL] + 2[V_2L_2] = K_1[V_i][L] + 2K'_2\, K_1^2[V_i]^2[L]^2 \qquad (5)$$

where L = ligand.

By rearranging equation 4 and substituting into equation 5, equation 6 is obtained

$$[VL]+2[V_2L_2] = K_1[V_4]^{1/4}K_4^{-1/4}[L]+2K'_2\, K_1^2\, ([V_4]^{1/4}\, K_4^{-1/4})^2\, [L]^2 \qquad (6)$$

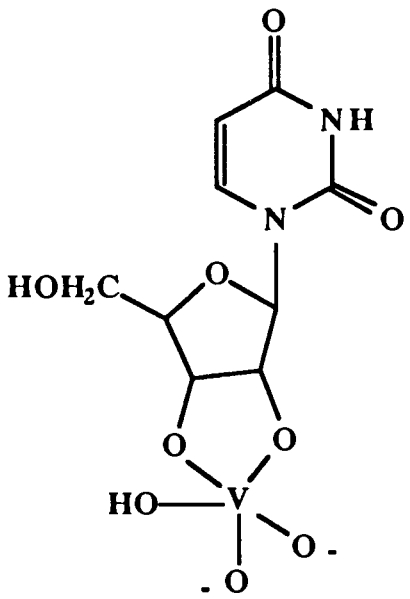

uridine-vanadate complex

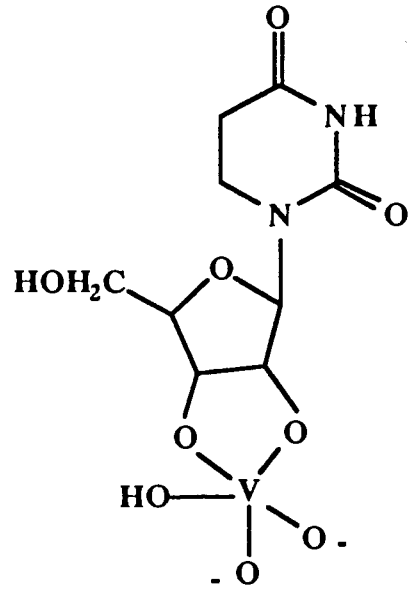

5,6-dihydrouridine-vanadate complex

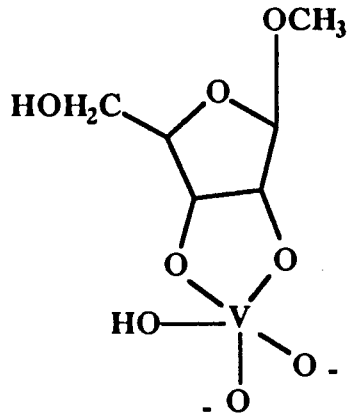

methyl β-D-ribofuranoside-vanadate complex

Fig. II.1

Proposed structures of the vanadate mononuclear complexes with uridine, 5,6-dihydrouridine and methyl β-D-ribofuranoside

Equation 6 defines a curve because both $[V_4]$ and [L] which are variables, are part of the intercept. Dividing through by $[V_4]^{1/4}\ K_4^{-1/4}[L]$, however, gives a linear equation, equation 7.

$$\frac{[VL]+2[V_2L_2]}{[V_4]^{1/4}K_4^{-1/4}[L]} = 2K'_2\ K_1^2\ K_4^{-1/4}\ [V_4]^{1/4}[L] + K_1 \qquad (7)$$

A value of $6.3 \times 10^9\ M^{-3}$ for K_4 (as defined by equation 4) was used in order to obtain the points to be plotted. This value was obtained from ^{51}V NMR spectra of the same vanadate solutions used for ligand titration, in the absence of ligand. The area of the signals at -560 and -576 ppm corresponding to free monomeric and tetrameric vanadate were measured in order to calculate the concentration of these species. K_4 value was obtained according to equation 4.

By plotting the data points in this way (equation 7), it is easier to extrapolate to the y intercept to determine whether K_1 has a measurable value. A graphical representation of this analysis is shown in Fig. II.2.1, II.2.2 and II.2.3a for the uridine, 5,6-dihydrouridine and methyl β-D-ribofuranoside ligands respectively. When the ligand titration was performed using a lower total vanadate concentration (less than 1 mM), the $[V_i]$ was obtained by measuring the area of the signal corresponding to monomeric vanadate, and subtracting the amount of vanadate esters present under this signal. The difference is the concentration of free V_i. In calculating the amount of vanadate esters present, an overall

II.2

Dependence of the equilibrium concentrations of vanadate complex upon varying concentrations of ligands

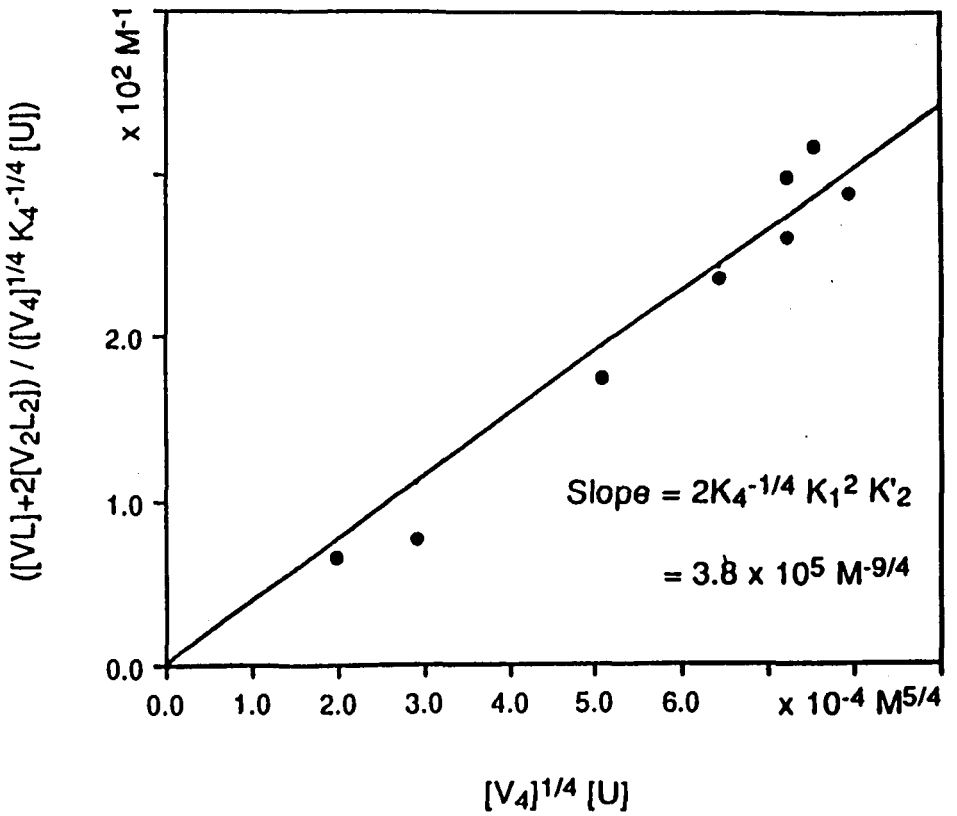

Fig. II.2.1

Plot of $([VL] + 2[V_2L_2])/([V_4]^{1/4} K_4^{-1/4} [U])$ versus $[V_4]^{1/4} [U]$: Determination of the equilibrium constants K_1 and $K'_2 K_1^2$ (K_3) for formation of mononuclear (1:1) uridine-vanadate complex and binuclear (2:2) uridine-vanadate complex. The slope gives $K'_2 K_1^2$ (K_3). Conditions were 5.0 mM Tris buffer, 0.35 M ionic strength with added KCl and 1.0 mM vanadate, pH 7.0. The range of uridine concentration used was 0-21 mM.

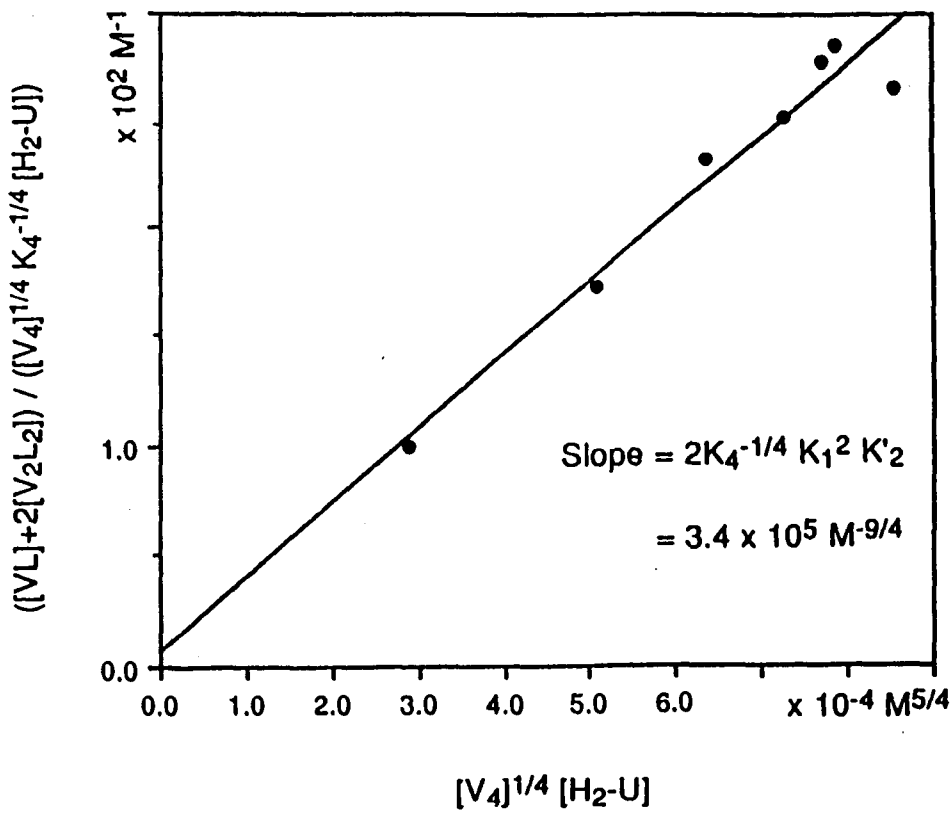

Fig. II.2.2

Plot of ([VL] + 2 $[V_2L_2]$)/($[V_4]^{1/4}$ $K_4^{-1/4}$ $[H_2\text{-}U]$) versus $[V_4]^{1/4}$ $[H_2\text{-}U]$: Determination of the equilibrium constants K_1 and K'_2 K_1^2 (K_3) for formation of mononuclear (1:1) 5,6-dihydrouridine-vanadate complex and binuclear (2:2) 5,6-dihydrouridine-vanadate complex. The slope gives K'_2 K_1^2 (K_3). Conditions were 5.0 mM Tris buffer, 0.35 M ionic strength with added KCl and 1.0 mM vanadate, pH 7.0. The range of 5,6-dihydrouridine concentration used was 0-21 mM.

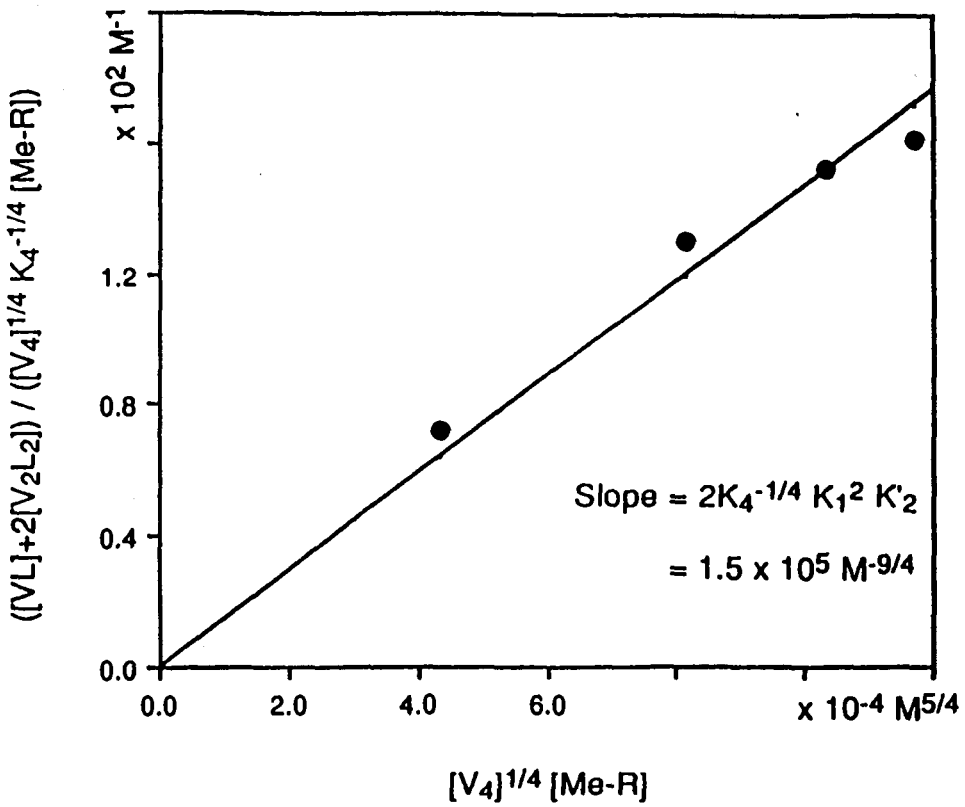

Fig II.2.3a

Plot of ([VL] + 2 [V_2L_2])/([V_4]$^{1/4}$ $K_4^{-1/4}$ [Me-R]) versus [V_4]$^{1/4}$ [Me-R]: Determination of the equilibrium constants K_1 and K'_2 K_1^2 (K_3) for formation of mononuclear (1:1) methyl β-D-ribofuranoside-vanadate complex and binuclear (2:2) methyl β-D-ribofuranoside-vanadate complex. The slope gives K'_2 K_1^2 (K_3). Conditions were 5.0 mM Tris buffer, 0.35 M ionic strength with added KCl and 1.0 mM vanadate, pH 7.0. The range of methyl β-D-ribofuranoside-vanadate concentration used was 0-20 mM.

equilibrium constant of 4 M^{-1} (40) was used. This equilibrium constant is the sum of the equilibrium constants for formation of acyclic and cyclic tetrahedral vanadate esters (40). So, by taking into account equation 5 again and dividing it by $[V_i]$ [L], the following is obtained:

$$\frac{[VL]+2[V_2L_2]}{[V_i][L]} = 2K'_2 K_1^2 [V_i][L]+K_1 \qquad (8)$$

Fig. II.2.3b shows a plot of the experimental values, according to this equation. Tables II.1, II.2 and II.3 show the distribution of the vanadate species of interest in the presence of these ligands. Table II.4 lists the different equilibrium constants obtained, K_1 which is the equilibrium constant for formation of VL and K_3 which is the overall equilibrium constant for formation of V_2L_2. K_3 is related to K_1 and K'_2 by the following equation,

$$K_3 = K_1^2 K'_2 \qquad (9)$$

A small shoulder appearing upfield from the signal at -522 to -525 ppm suggests the presence of another compound, probably also with a trigonal bipyramidal geometry due to its proximity, to which it is not yet possible to assign a chemical structure. This shoulder is more obvious in the vanadate-5,6-dihydrouridine system.

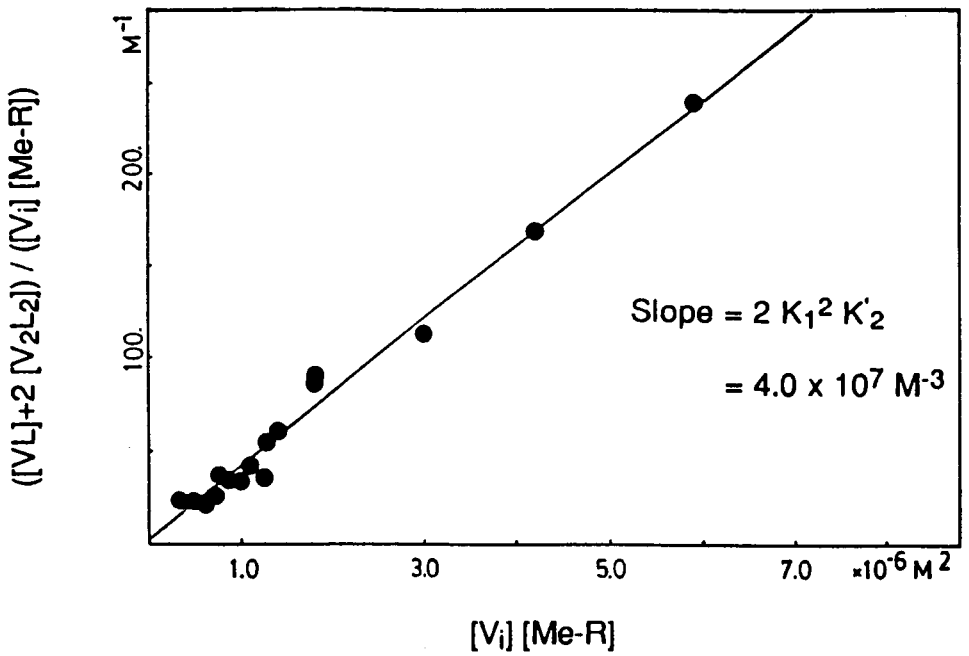

Fig. II.2.3b

Plot of ([VL] + 2 $[V_2L_2]$)/([V_i] [Me-R]) versus [V_i] [Me-R]: Determination of the equilibrium constants K_1 and K'_2 K_1^2 (K_3) for formation of mononuclear (1:1) methyl β-D-ribofuranoside-vanadate complex and binuclear (2:2) methyl β-D-ribofuranoside-vanadate complex. The slope gives K'_2 K_1^2 (K_3) and the y intercept gives K_1, as shown in equation 8. Conditions were 5.0 mM Tris buffer, 1.0 M ionic strength with added KCl, pH 7.5. The range of vanadate concentration used was 0.05-2.00 mM, the range of methyl β-D-ribofuranoside-vanadate concentration used was 4-300 mM.

Table II.1

Distribution of the vanadate species of interest as a function of the concentration of uridine

$[U_t]$ (x 10^{-3} M)	$[V_i]$ (x 10^{-3} M)	$[V_4]$ (x 10^{-3} M)	[-523] (x 10^{-3} M)*
0.0	0.352	0.108	0.000
1.0	0.350	0.110	0.000
2.0	0.341	0.108	0.046
3.0	0.340	0.098	0.080
6.0	0.309	0.064	0.315
9.0	0.262	0.033	0.540
12.1	0.215	0.016	0.673
15.1	0.181	0.006	0.767
18.1	0.144	0.004	0.816
21.1	0.124	0.002	0.853

* Vanadium atom concentration.
Concentration of total vanadium = 1.0 mM. Conditions were 5.0 mM Tris buffer, 0.35 M ionic strength with added KCl, pH 7.0. $[U_t]$ = total uridine concentration, $[V_i]$ = monovanadate concentration, $[V_4]$ = tetravanadate concentration, [-523] = sum of the concentrations of VL and V_2L_2.

Table II.2

Distribution of the vanadate species of interest as a function of the concentration of 5,6-dihydrouridine

$[H_2\text{-}U_t]$ ($\times 10^{-3}$ M)	$[V_i]$ ($\times 10^{-3}$ M)	$[V_4]$ ($\times 10^{-3}$ M)	[-522] ($\times 10^{-3}$ M)*
0.0	0.363	0.112	0.000
3.0	0.354	0.099	0.104
6.0	0.312	0.063	0.308
9.0	0.273	0.032	0.522
12.0	0.237	0.017	0.648
14.9	0.193	0.008	0.746
18.0	0.168	0.004	0.792
21.0	0.157	0.003	0.804

* Vanadium atom concentration.
Concentration of total vanadium = 1.0 mM. Conditions were 5.0 mM Tris buffer, 0.35 M ionic strength with added KCl, pH 7.0. $[H_2\text{-}U_t]$ = total 5,6-dihydrouridine concentration.

Table II.3a

Distribution of the vanadate species of interest as a function of the concentration of methyl β-D-ribofuranoside

[Me-R_t] (x 10^{-3} M)	[V_i] (x 10^{-3} M)	[V_4] (x 10^{-3} M)	[-523] (x 10^{-3} M)*
0.0	0.368	0.115	0.000
4.5	0.340	0.098	0.112
10.0	0.314	0.052	0.380
15.0	0.262	0.026	0.562
20.0	0.222	0.014	0.675

* Vanadium atom concentration.
Concentration of total vanadium = 1.0 mM. Conditions were 5.0 mM Tris buffer, 0.35 M ionic strength with added KCl, pH 7.0. [Me-R_t] = total methyl β-D-ribofuranoside concentration.

Table II.3b

Distribution of the vanadate species as a function of the concentration of methyl β-D-ribofuranoside and total vanadate

$[V_t]$ (x 10^{-3} M)*	$[Me\text{-}R_t]$ (x 10^{-3} M)	$[V_i]$ (x 10^{-3} M)	$[V_{2t} + V_4]$ (x 10^{-3} M)*	[-523] (x 10^{-3} M)*
0.10	4.0	0.091	0.008	0.000
0.10	6.0	0.085	0.005	0.008
0.10	8.3	0.079	0.008	0.010
0.10	11.7	0.072	0.005	0.020
0.10	16.7	0.064	0.004	0.028
0.10	25.0	0.049	0.002	0.045
0.10	50.0	0.025	0.000	0.070
0.10	80.0	0.015	0.000	0.080
0.20	50.0	0.035	0.000	0.158
0.05	50.0	0.017	0.000	0.030
0.25	300.0	0.004	0.000	0.024
0.50	300.0	0.007	0.000	0.048
1.00	300.0	0.010	0.000	0.098
0.10	25.0	0.040	0.003	0.052
0.25	25.0	0.069	0.011	0.164
0.50	25.0	0.105	0.026	0.359
1.00	25.0	0.162	0.105	0.717
2.00	25.0	0.231	0.322	1.425
0.05	25.0	0.027	0.001	0.019

* Vanadium atom concentration.
Conditions were 5.0 mM Tris buffer, 1.0 M ionic strength with added KCl, pH 7.5. $[V_t]$ = total vanadate concentration, $[V_{2t} + V_4]$ = sum of the concentrations of total divanadate and tetravanadate.

In Table II.4, K_1 and K_3 for complexation between vanadate and methyl β-D-ribofuranoside were determined under two different conditions. The value of the equilibrium constant for formation of the vanadate binuclear complex (K_3) does not change significantly upon increasing the ionic strength from 0.35 M to 1.0 M and increasing the pH from 7.0 to 7.5, indicating that the formation of vanadate binuclear complex is relatively insensitive to ionic strength and pH, at least under these conditions.

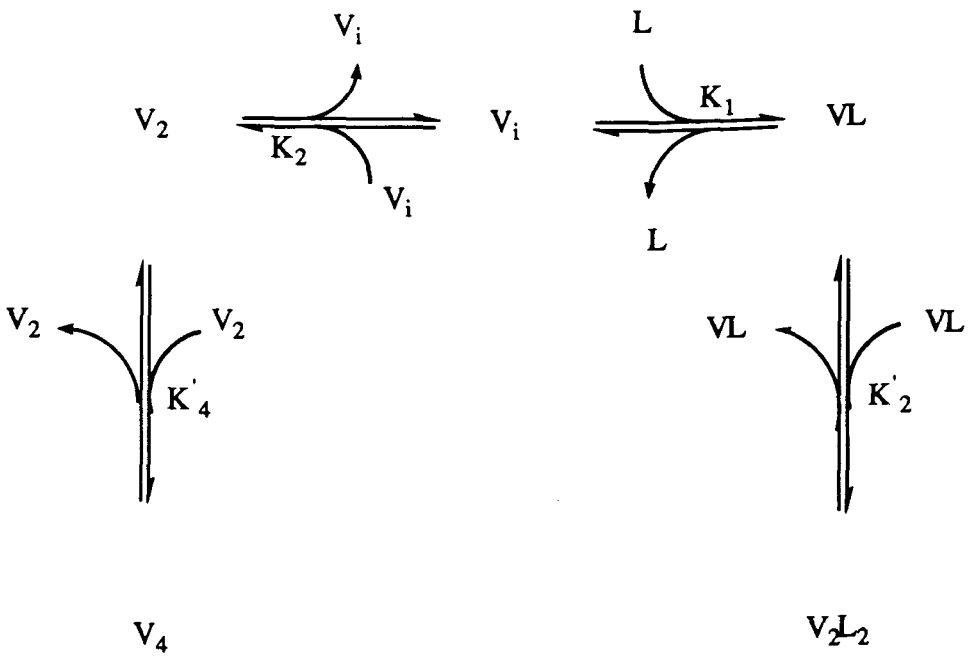

(II.3)

However, nothing can be concluded about the dependence of K_1 on ionic strength and pH, due to the difficulty in obtaining an accurate

Table II.4

Equilibrium constants of various vanadate-ligand complexes determined from NMR studies

Ligand	K_1 (M^{-1})	K_3 (M^{-3})
uridine	____ [a]	$(5.3 \pm 0.2) \times 10^7$ [b,c]
5,6-dihydrouridine	____ [a]	$(4.8 \pm 0.4) \times 10^7$ [b,c]
methyl β-D-ribofuranoside	____ [a]	$(2.1 \pm 0.1) \times 10^7$ [b,c]
	1.8 ± 1.5 [d]	$(2.0 \pm 0.1) \times 10^7$ [c,e]

[a] K_1 was not detected within experimental error.
[b] Conditions were 5.0 mM Tris buffer, 0.35 M ionic strength with added KCl, pH 7.0.
[c] The error was obtained using the least-squares method.
[d] A high standard deviation is due to the difficulty in detecting VL.
[e] Conditions were 5.0 mM Tris buffer, 1.0 M ionic strength with added KCl, pH 7.5.

small value. Scheme II.3 shows the different equilibria that exist in a vanadate solution under the conditions described in Table II.4.

II.2. Ultraviolet Absorption Spectrophotometry

The aqueous chemistry of vanadium as well as the other metals of Group VB in the periodic table has been known to be rather complicated. Vanadium can exist in solution as a mixture of different species such as monomeric vanadate ($H_2VO_4^-$, HVO_4^{2-}), dimeric vanadate, tetrameric vanadate, decavanadate, etc. However, at neutral pH, and concentrations up to 0.1 mM, vanadium(V) exists almost completely as the $H_2VO_4^-$ species.

Ultraviolet and visible spectrophotometry have been widely used for the quantitative determination of substances. The advantage of spectrophotometric methods over NMR methods is that under appropriate conditions the former can detect minute quantities of a material in a mixture of two or more materials. Frequently, two compounds or two isomers of a compound existing in equilibrium exhibit overlapping absorption bands. In many cases, because of the higher sensitivity obtained by spectrophotometric methods, it is possible to determine the number and identity of the compounds present in solution.

Vanadium(V) oxoanions are colourless, however, the UV absorption spectra of this transition metal ion and many of its complexes is composed of charge-transfer bands which are fairly intense (41). In this work, ultraviolet spectrophotometry has been

shown to be a useful tool to investigate the reaction of vanadate with methyl β-D-ribofuranoside.

II.2.1. Experimental procedure

II.2.1.1. Preparation of samples

Solutions were prepared by mixing appropriate amounts of the stock solutions to obtain final concentrations of 5.0 mM Tris buffer, 0.35 M KCl and 9.62 x 10^{-2} mM vanadate. Formation of decavanadate occurs in acidic conditions. To avoid the use of HCl to adjust the pH, the vanadate stock solution was added to the Tris buffer-KCl mixture which pH was 6.8. Then the pH was adjusted to 7.0 using small aliquots of NaOH.

II.2.1.2. Instrumentation

Spectra were recorded from 210 to 820 nm on a Hewlett Packard 8452A diode array spectrophotometer. The signal averaging time was 25.5 s for each spectrum, i.e., each spectrum was the average of 255 spectra. An internal reference procedure which utilized the absorbance from 624 nm to 634 nm was applied to each spectrum for baseline correction.

II.2.1.3. Ligand titration and absorbance measurement

2.0 ml of the 9.62 x 10^{-2} mM vanadate mixture was placed into a 3 ml UV cell containing a small magnetic stir bar. The

sample was temperature equilibrated at 25 °C for 5 min. before recording the first spectrum. A Hamilton syringe was used to add aliquots of a buffered solution of methyl β-D-ribofuranoside, pH 7.0. After each addition, the sample was temperature equilibrated and a spectrum was recorded.

In order to correct for the small absorbance of methyl β-D-ribofuranoside, a spectrum of the stock solution (1.01 M) was recorded and the extinction coefficient was calculated. The E_{270} was 0.145 $M^{-1}\,cm^{-1}$. Using this value, the absorbance at 270 nm, resulting from the presence of methyl β-D-ribofuranoside, was calculated and subtracted from the observed absorbance (equation 10).

$$A_{calc} = A_{obs} - A_{Me\text{-}R} \qquad (10)$$

where A_{calc} = calculated absorbance, A_{obs} = observed absorbance, and $A_{Me\text{-}R}$ = methyl β-D-ribofuranoside absorbance.

II.2.2. Results and discussion: Complexation of vanadium(V) and methyl β-D-ribofuranoside

The addition of aliquots of methyl β-D-ribofuranoside to a vanadate solution generates the family of spectra shown in Fig. II.3. The λ max is very close to that of vanadate, but the extinction coefficient of the vanadate complexed to methyl β-D-ribofuranoside is greater. A plot of the absorbance at 270 nm versus the

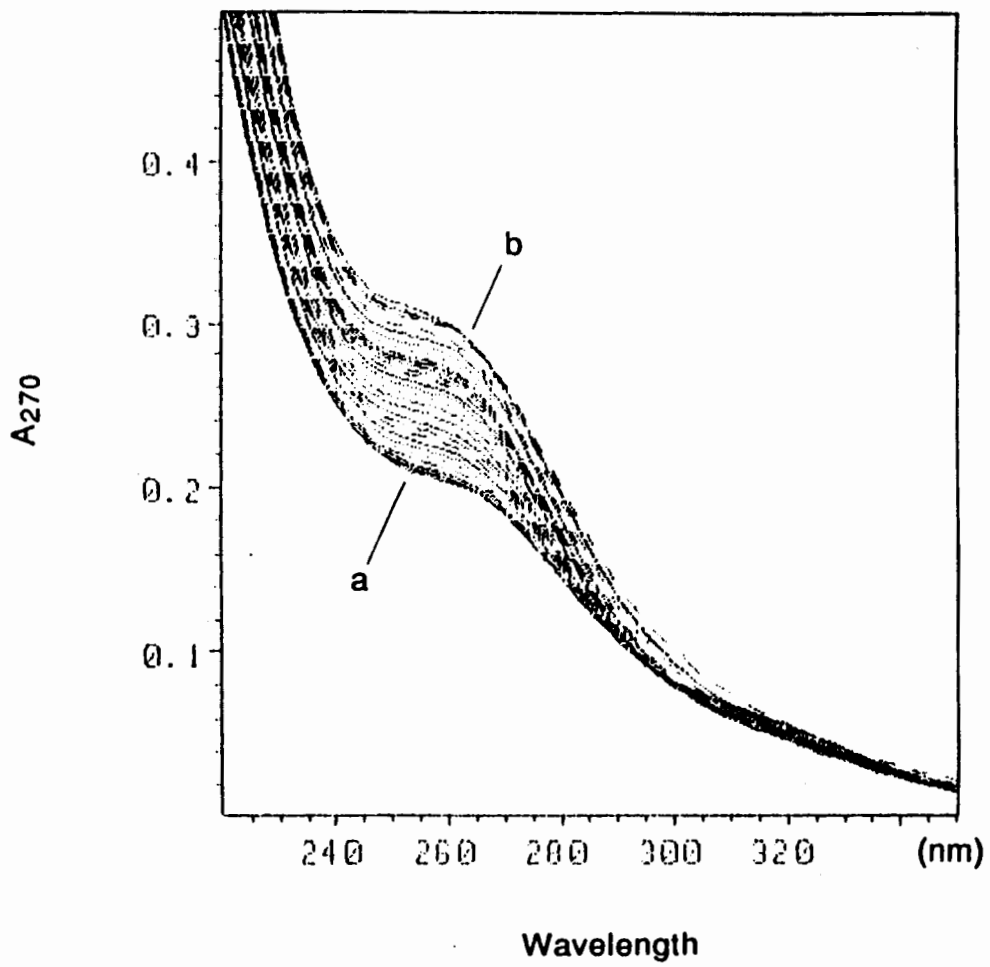

Fig. II.3

Ultraviolet spectra of vanadate at various concentrations of methyl β-D-ribofuranoside. Conditions were 5.0 mM Tris buffer, 0.35 M KCl and 0.1 mM total vanadate, at pH 7.0 and 25 °C.

concentration of methyl β-D-ribofuranoside shows a curve with a slight sigmoidal shape. In an initial analysis of this curve, only the reaction described in equation 3 was assumed to take place, that is

$$2\ V_i + 2L \xrightleftharpoons{K_3} V_2L_2 \qquad [V_i]^2\,[L]^2\,K_3 = [V_2L_2]$$

The following conservation equations were considered:

$$A_t = E_{Vi}\,[V_i] + E_{V2L2}\,[V_2L_2] \tag{11}$$

$$[V_t] = [V_i] + 2[V_2L_2] \tag{12}$$

$$[L_t] = [L] + 2[V_2L_2] \tag{13}$$

where A_t = total absorbance, E_{Vi} = inorganic vanadate extinction coefficient at 270 nm, E_{V2L2} = (2:2) vanadate-ligand complex extinction coefficient at 270 nm, $[V_t]$ = total vanadate concentration, $[L_t]$ = total ligand concentration, and [L] = free ligand concentration. At the concentration range studied, $[V_2L_2]$ is very small compared to [L], therefore [L] can be approximated to $[L_t]$, i.e.,

$$[L_t] = [L] \tag{13a}$$

On combination of equation 3 with the conservation equations, eq. 11, 12 and 13a, equation 14 was obtained.

$$A_t = E_{Vi}\left(\frac{-1+\sqrt{1+8K_3[L]^2[V_t]}}{4K_3[L]^2}\right) +$$

$$E_{V2L2}\,K_3\,[L]^2\left(\frac{-1+\sqrt{1+8K_3[L]^2[V_t]}}{4K_3[L]^2}\right)^2 \qquad (14)$$

This equation was utilized in a standard non-linear regression program (BMDP) to generate a curve, using the known value for E_{Vi} = 1,700 $M^{-1}\,cm^{-1}$. The refinement gave the extinction coefficient E_{V2L2} = 5,350 ± 35 $M^{-1}\,cm^{-1}$ and $K_3 = (2.1 \pm 0.1) \times 10^7$ M^{-3}. Examination of the results showed that a good fit to the experimental data was obtained. The value obtained for K_3 was the same as that determined previously from the NMR study.

In order to determine whether the presence of the monomer, VL, is negligible or not, modification of the conservation equations to include formation of VL, eq. 11-13, gave equations 15-17,

$$A_t = E_{Vi}[V_i] + E_{VL}[VL] + E_{V2L2}[V_2L_2] \qquad (15)$$

$$[V_t] = [V_i] + [VL] + 2[V_2L_2] \qquad (16)$$

$$[L_t] = [L] + [VL] + 2[V_2L_2] \qquad (17)$$

where E_{VL} = (1:1) vanadate-ligand complex extinction coefficient at 270 nm, when the additional equilibrium of equation 1 was considered.

$$V_i + L \xrightleftharpoons{K_1} VL \qquad [V_i]\,[L]\,K_1 = [VL]$$

Again, at the concentration range studied, $[V_2L_2]$ and [VL] are very small compared to [L], therefore [L] can be approximated to $[L_t]$, i.e.,

$$[L_t] = [L] \tag{17a}$$

Combination of equation 1 with the conservation equations, eq. 15, 16 and 17a, gave the final equation, eq. 18.

$$A_t = (E_{Vi} + E_{VL}\,K_1\,[L]) \left(\frac{-1-K_1[L]+\sqrt{(1+K_1[L])^2+8K_3[L]^2[V_t]}}{4K_3[L]^2}\right)$$

$$+ (E_{V2L2}\,K_3\,[L]^2) \left(\frac{-1-K_1[L]+\sqrt{(1+K_1[L])^2+8K_3[L]^2[V_t]}}{4K_3[L]^2}\right)^2 \tag{18}$$

The two parameters, E_{VL} and K_1, were then allowed to vary simultaneously in the least-squares program. The initial estimate for E_{VL} value was 2,675 $M^{-1}\,cm^{-1}$ (i.e., 1/2 E_{V2L2}) and that for K_1 value was 0.5 M^{-1} (the reported value of the equilibrium constant for formation of a pentacoordinate vanadate-lactate complex (4)). The values obtained for E_{VL} and K_1 were 2,550 ± 220 $M^{-1}\,cm^{-1}$ and 1.1 ± 0.9 M^{-1}, respectively.

There is a correlation between K_1 and K_3. In an effort to examine this problem more closely, the lower limiting K_3 value obtained from the NMR study (2.0×10^7 M^{-3}) was assumed for the UV analysis. Figures II.4.1a, II.4.2a and II.4.3a show the

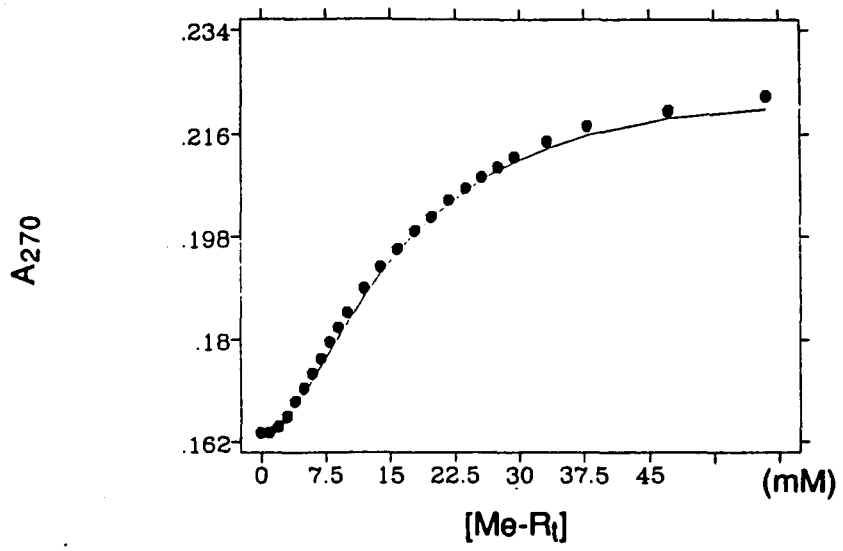

Fig. II.4.1a

Plot of the absorbance of vanadate at 270 nm as a function of the total methyl β-D-ribofuranoside concentration. Comparison of the experimental values and a calculated curve assuming only the formation of V_2L_2. The curve is described by equation 14. $K_1 = 0$, $K_3 = 2.0 \times 10^7\ M^{-3}$. Conditions were 5.0 mM Tris buffer, 0.35 M ionic strength with added KCl and 0.1 mM total vanadate, at pH 7.0 and 25 °C

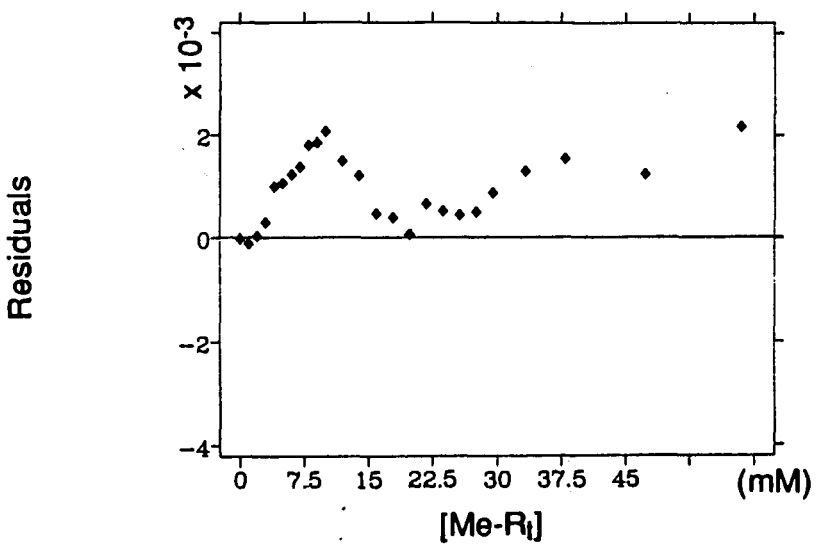

Fig. II.4.1b

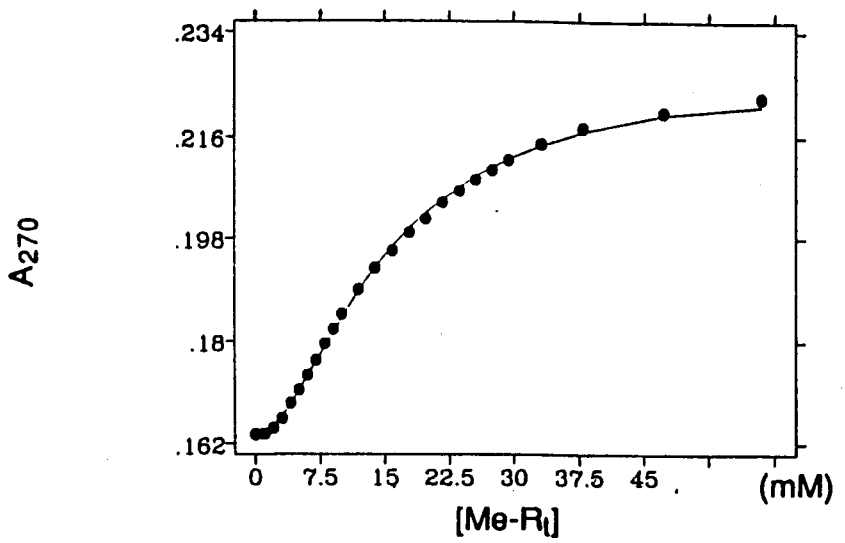

Fig. II.4.2a

Plot of the absorbance of vanadate at 270 nm as a function of the total methyl β-D-ribofuranoside concentration. Comparison of the experimental values and a calculated curve assuming the formation of VL and V_2L_2. The curve is described by equation 18. $K_1 = 1.8 \pm 0.8$ M^{-1}, $K_3 = 2.0 \times 10^7$ M^{-3}. Conditions were 5.0 mM Tris buffer, 0.35 M ionic strength with added KCl and 0.1 mM total vanadate, at pH 7.0 and 25 °C.

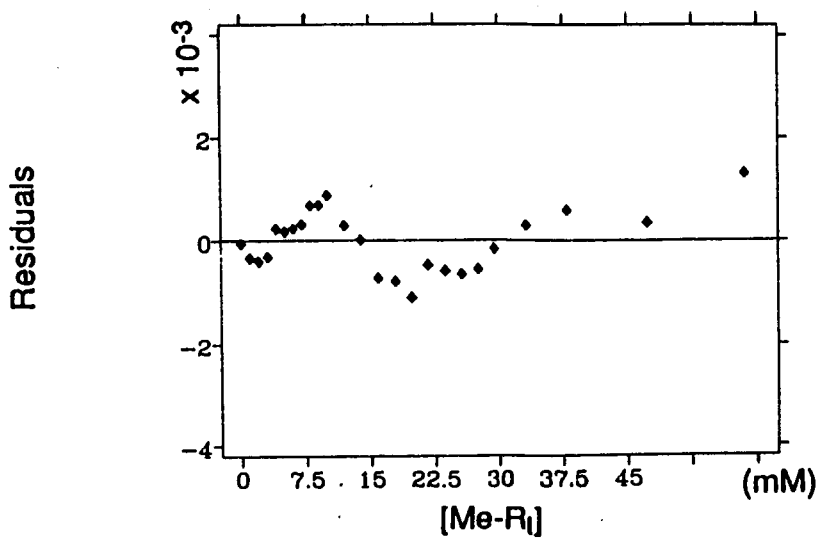

Fig. II.4.2b

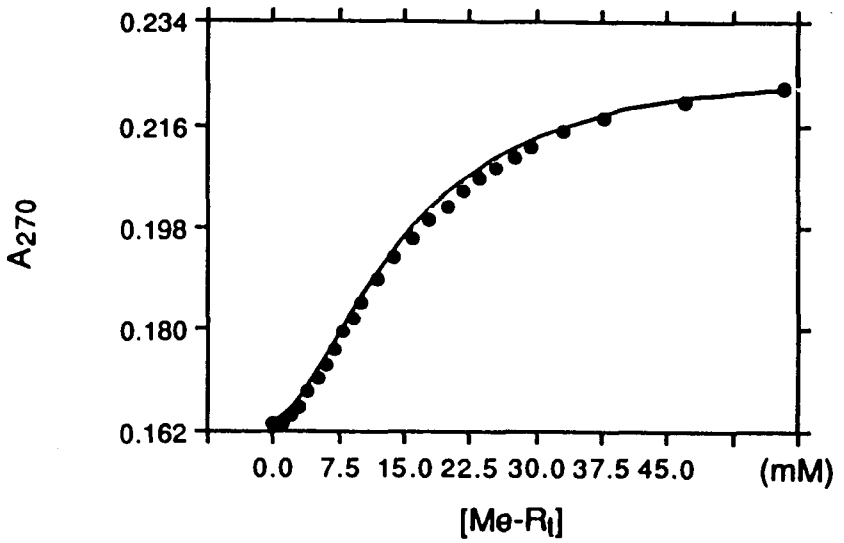

Fig. II.4.3a

Plot of the absorbance of vanadate at 270 nm as a function of the total methyl β-D-ribofuranoside concentration. Comparison of the experimental values and a calculated curve assuming formation of VL and V_2L_2 using an upper limit of 2 standard deviations for K_1. The curve is described by equation 18. K_1 = 3.4 M^{-1}, K_3 = 2.0 x 10^7 M^{-3}. Conditions were 5.0 mM Tris buffer, 0.35 M ionic strength with added KCl and 0.1 mM total vanadate, at pH 7.0 and 25 °C.

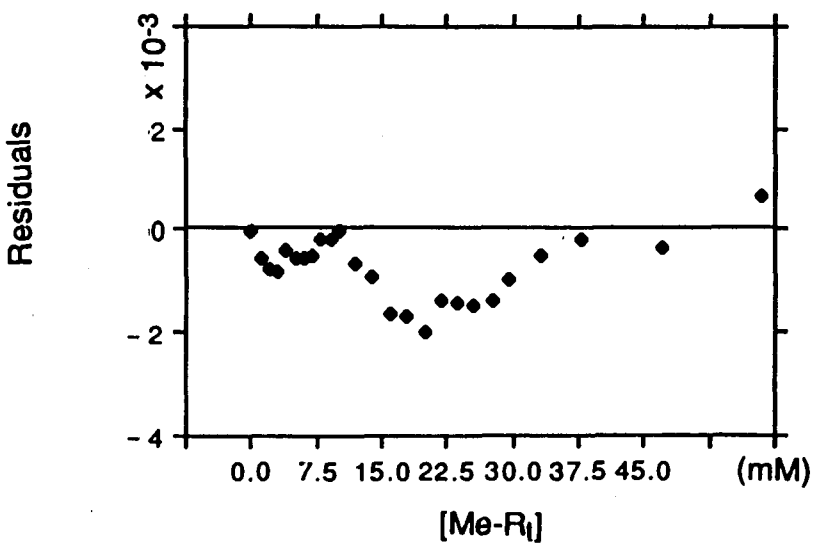

Fig. II.4.3b

calculated curves corresponding to different analysis. Fig. II.4.1a shows a plot of the experimental points with a calculated curve, using a value of E_{V2L2} = 5,350 M^{-1} cm^{-1} as determined from the refinement and the lower limit for $K_3 = 2.0 \times 10^7$ M^{-3}. Fig. II.4.2a shows a plot of the same experimental points with a calculated curve, using the previous values of E_{V2L2} and K_3, and values for E_{VL} and K_1 of 2,820 M^{-1} cm^{-1} and 1.8 M^{-1}, respectively. Fig. II.4.3a shows a comparison between the same experimental points and a calculated curve assuming the same values for E_{V2L2}, E_{VL} and K_3, and an upper limit of 2 standard deviations for K_1 = 3.4 M^{-1}.

Residual plots, where the y value of each point is replaced by the distance of that point from the curve, are useful graphical representations of the validity of an equation. If the parameters are appropriate to describe the curve, a residual plot will show random residual plots; whereas if they are inappropriate, the residuals will have a systematic relationship with the x values (42). Fig II.4.1b, II.4.2b and II.4.3b show residual plots for the different analyses. As can be seen in Fig. II.4.1b, the residuals were consistently positive when the presence of VL was neglected; when a value of 3.4 M^{-1} for K_1 was fixed, the residuals were consistently negative (Fig. II.4.3b) indicating that this value overestimates the [VL] in the system. However, when K_1 was assumed to be 1.8 M^{-1}, random residuals were obtained as shown in Fig. II.4.2b. It is noteworthy to point out that the value determined for K_1 is not

accurate since VL is present in small concentrations relative to V_2L_2. However, it is clear that a significant improvement in the fit of the calculated line to the data can be achieved if it is assumed that the product VL is formed with $K_1 = 1.8\ M^{-1}$, an extinction coefficient equal approximately to half the extinction coefficient of the binuclear complex and a lower limit value for $K_3 = 2.0 \times 10^7\ M^{-3}$. The purpose of these plots is only to show that the presence of VL should not be neglected and that the value of K_1 is very small.

The value of K_1 is very sensitive to the value of K_3. From the NMR study, the best value for K_3 was $(2.1 \pm 0.1) \times 10^7\ M^{-3}$, so when K_3 was fixed to its lower limit ($2.0 \times 10^7\ M^{-3}$), the refined value for K_3 was $1.8 \pm 0.8\ M^{-1}$. When K_3 was fixed to its upper limit ($2.2 \times 10^7\ M^{-3}$), the refined value for K_1 was $0.4\ M^{-1}$. And when K_3 was fixed to its best value ($2.1 \times 10^7\ M^{-3}$), the refined value for K_1 was $1.1 \pm 0.9\ M^{-1}$. Finally, the best fit to the experimental data was obtained when E_{V2L2} and K_3 values were fixed to $5{,}350\ M^{-1}\ cm^{-1}$ and $2.1 \times 10^7\ M^{-3}$, respectively, and E_{VL} and K_1 values were refined to obtain values of $2{,}550 \pm 220\ M^{-1}\ cm^{-1}$ and $1.1 \pm 0.9\ M^{-1}$, respectively. In all cases where VL was assumed to be present, the root mean square was approximately 10 times smaller than when VL was neglected.

The values for K_1 ($1.1\ M^{-1}$) and K_3 ($2.1 \times 10^7\ M^{-3}$) obtained from these spectrophotometric experiments are in good agreement with the ones obtained from ^{51}V NMR studies for K_1 (1.8

M^{-1}) and K_3 (2.1×10^7 M^{-3}). Although the evidence for the existence of VL from either UV or ^{51}V NMR studies is indirect, the K_1 values obtained using these two different approaches are in very good agreement within experimental error. These results provide strong support for the existence of minute quantities of VL in a solution where the main product is V_2L_2.

Chapter III
Biochemistry of Vanadium(V) Complexes

III.1. ^{51}V NMR Spectroscopy: Binding of Vanadate Complexes to RNase A

III.1.1. Experimental procedure

III.1.1.1. Preparation of RNase A samples for ^{51}V NMR spectroscopy

RNase A samples were prepared by dissolving the lyophilized powder in a solution containing 5.0 mM Tris and 0.35 M KCl, the pH was adjusted to approximately 7 with small aliquots of 0.05 N NaOH, and then an appropriate quantity of vanadate was added to give a final concentration of 1.0 mM. The pH was adjusted again to 7.0 before bringing the solution to the final volume. This procedure avoided the formation of decavanadate which is an oligomer that hydrolyses very slowly at neutral pH.

A small aliquot was withdrawn from the enzyme solution before addition of vanadate, in order to determine the protein concentration by UV spectrophotometry ($E^{1\%}_{280}$ = 7.3, MW = 13,700 (43)). It was done in this way because vanadate interfered with the absorption spectrum of RNase A. Samples of 2.0 mL. were used for the NMR spectroscopy.

Stock solutions of uridine, 5,6-dihydrouridine and methyl β-D-ribofuranoside were prepared as described in Section II.1.1.2.

III.1.1.2. Studies of the binding of vanadate-ligand complexes to RNase A

A V(V)-H_2O_2 complex was used in order to provide an integral reference for the NMR spectra. This material was used because it gives rise to NMR signals that do not overlap with the vanadate signals of interest. The materials to be studied were placed into a 10 mm diameter NMR tube. Then a capillary tube containing a solution of the V(V)-H_2O_2 complex was introduced into the sample tube. In this way, the reference solution is kept isolated from the sample solution and simultaneous spectra of sample and reference were obtained. It was not possible to detect any new signal due to a vanadate-ligand-enzyme complex. Since the ^{51}V nucleus has a large quadrupole moment, and because the bound vanadate tumbles at the same rate as the enzyme, vanadate bound to the enzyme is expected to give a very broad signal which can be lost in the baseline of the ^{51}V NMR spectrum. Therefore, in order to determine the amount of vanadate bound to the enzyme, the area of the signals corresponding to the free species was measured, and the difference from the total vanadium atom concentration gives the concentration of vanadate complex bound to the enzyme.

$$[V_b] = [V_t]-([VL]+2[V_2L_2]+[V_i]+2[V_2]+4[V_4]) \qquad (19)$$

where $[V_b]$ = concentration of vanadate bound to RNase A.

Conditions for these experiments were 5.0 mM Tris, 0.35 M ionic strength with added KCl and pH 7.0. The NMR samples consisted of an approximately 1:1 enzyme-vanadate solution and the concentration of the ligand was varied from 0-20 mM.

III.1.2. Results and discussion: Interaction of vanadate-ligand complexes with RNase A

The interaction of vanadate-ligand complexes (vanadate-uridine, vanadate-5,6-dihydrouridine and vanadate-methyl β-D-ribofuranoside) with RNase A was studied by ^{51}V NMR spectroscopy. The vanadate-uridine-RNase A system has been studied also by NMR spectroscopy by Borah et al (28). However, no quantitative experiments were performed in order to determine an approximate value of the binding constant of the (1:1) uridine-vanadate complex to RNase A.

A series of spectra is shown in Fig. III.1 and III.2. At low concentrations of uridine or 5,6-dihydrouridine, the signals near -523 ppm for the vanadate-uridine complex or the vanadate-5,6-dihydrouridine complex are not observed. However, it is evident that binding of vanadate-ligand complex to the enzyme has occurred since the total area of the signals of the free vanadate species has decreased. At the higher concentrations of uridine and 5,6-dihydrouridine, the signals due to the free vanadate complexes can be observed. Plots of the fraction of enzyme bound by a vanadate-

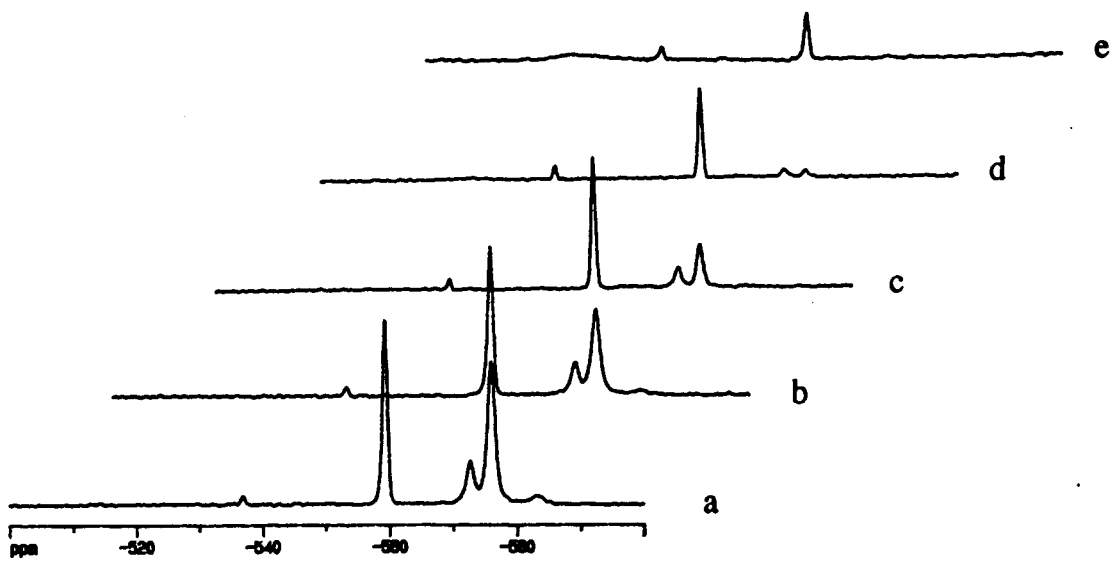

Fig. III.1

^{51}V NMR spectra: Binding of vanadate as a complex to RNase A as a function of the concentration of uridine. Conditions were 1.0 mM vanadate, 0.9 mM RNase A, 5.0 mM Tris buffer, 0.35 M KCl, pH 7.0. Spectra: a) No addition of uridine, b) + 0.3 mM uridine, c) + 1.0 mM, d) + 4.0 mM, e) + 11.7 mM.

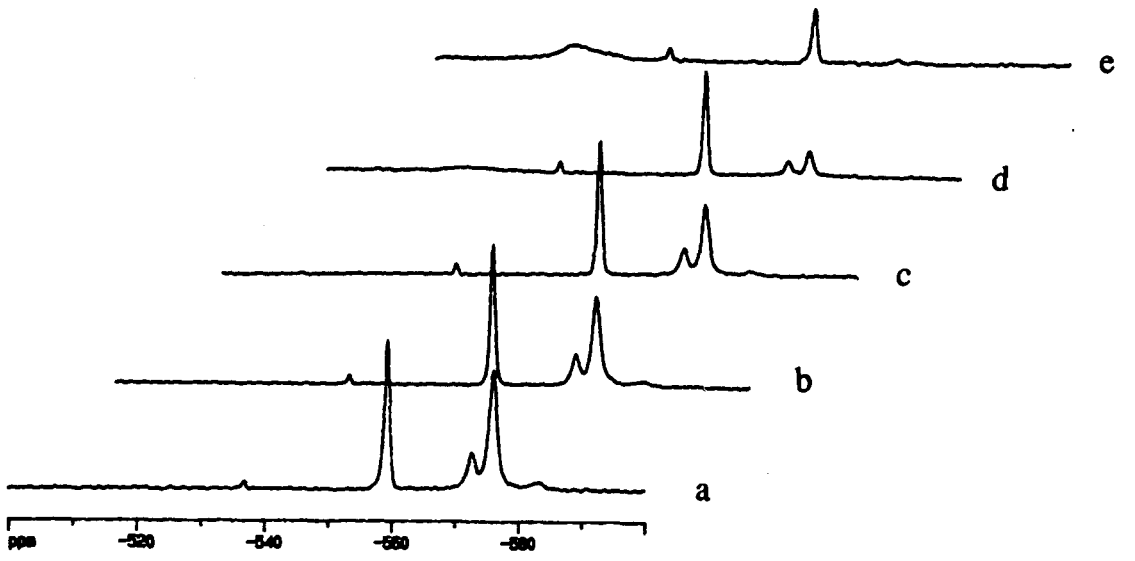

Fig. III.2

^{51}V NMR spectra: Binding of vanadate as a complex to RNase A as a function of the concentration of 5,6-dihydrouridine. Conditions were 1.0 mM vanadate, 0.9 mM RNase A, 5.0 mM Tris buffer, 0.35 M KCl, pH 7.0. Spectra: a) No addition of 5,6-dihydrouridine, b) + 0.3 mM 5,6-dihydrouridine, c) + 1.1 mM, d) + 4.4 mM, e) + 12.8 mM.

ligand complex as a function of the total concentration of ligand are shown in Fig. III.3.1, III.3.2 and III.3.3. Analysis of these data was done by using the following conservation equations:

$$[E_t] = [E] + [E{\cdot}L] + [E{\cdot}VL] + [E{\cdot}V_i] \quad (20)$$

$$[V_t] = [V_i] + 2[V_2] + 4[V_4] + 2[V_2L_2] + [VL] + [E{\cdot}V_i] + [E{\cdot}VL] \quad (21)$$

$$[L_t] = [L] + [VL] + 2[V_2L_2] + [E{\cdot}VL] + [E{\cdot}L] \quad (22)$$

where $[E_t]$ = total RNase A concentration, $[E]$ = free RNase A concentration, $[E{\cdot}L]$ = RNase A-ligand complex concentration, $[E{\cdot}VL]$ = RNase A-vanadate-ligand complex concentration, and $[E{\cdot}V_i]$ = RNase A-vanadate complex concentration, assuming that

$$[V_b] = [E{\cdot}VL] + [E{\cdot}V_i] \quad (23)$$

and including the following equilibria

$$2\ V_i \underset{}{\overset{K_2}{\rightleftharpoons}} V_2 \qquad K_2 = \frac{[V_2]}{[V_i]^2} \quad (24)$$

$$4\ V_i \underset{}{\overset{K_4}{\rightleftharpoons}} V_4 \qquad K_4 = \frac{[V_4]}{[V_i]^4} \quad (4)$$

$$V_i + L \underset{}{\overset{K_1}{\rightleftharpoons}} VL \qquad K_1 = \frac{[VL]}{[V_i][L]} \quad (1)$$

III.3

Dependence of the concentration of vanadate complex bound to RNase A upon varying concentrations of ligands

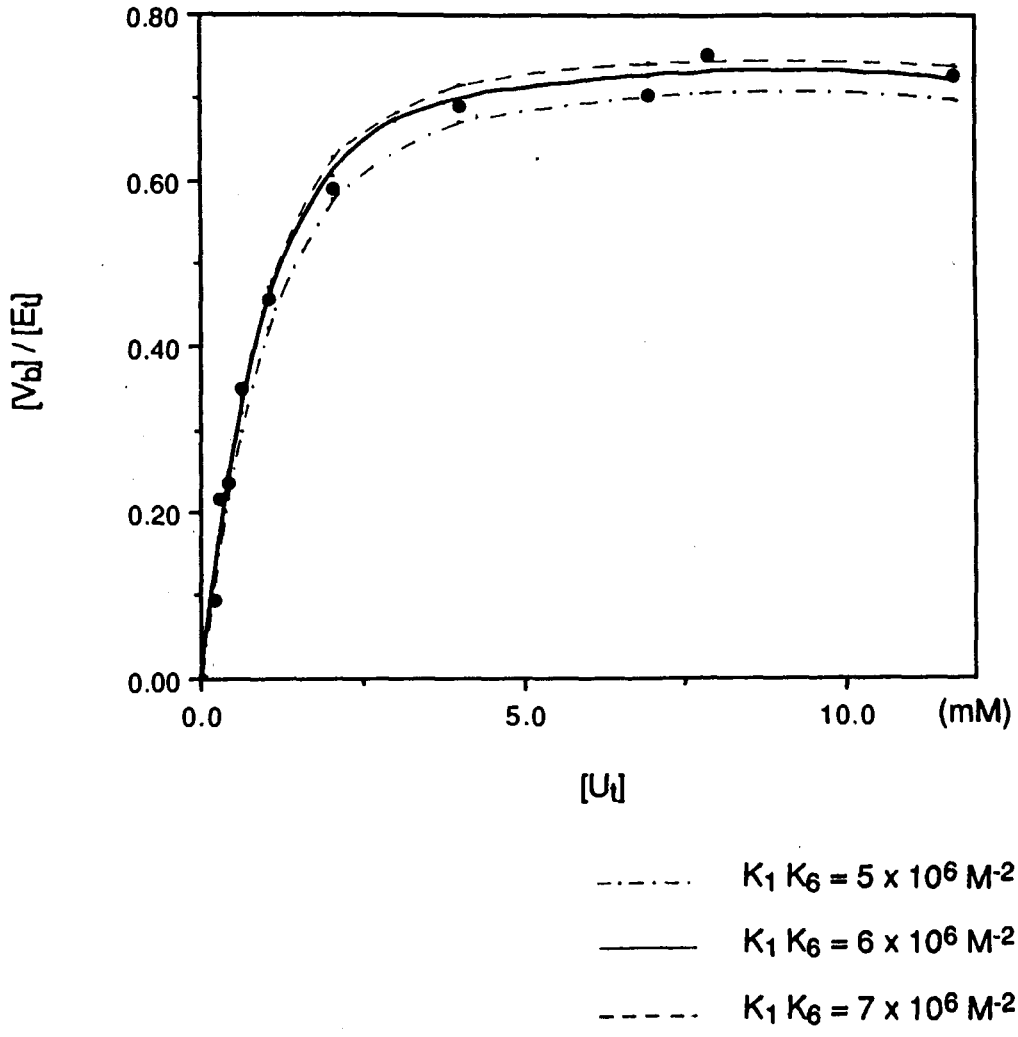

Fig. III.3.1

Plot of $[V_b]/[E_t]$ versus $[U_t]$: Determination of the value of the product of the equilibrium constants K_1K_6 (K_1 = formation constant of mononuclear (1:1) uridine-vanadate complex, K_6 = binding constant of (1:1) uridine-vanadate complex to RNase A). $K_1K_6 = (6 \pm 1) \times 10^6$ M^{-2}. The best fit was obtained when K_5 $(1/K_{iU}) = 1.25 \times 10^2$ M^{-1}. Conditions were 5.0 mM Tris buffer, 0.35 M KCl, 1 mM total vanadate and 0.9 mM total RNase A, pH 7.0.

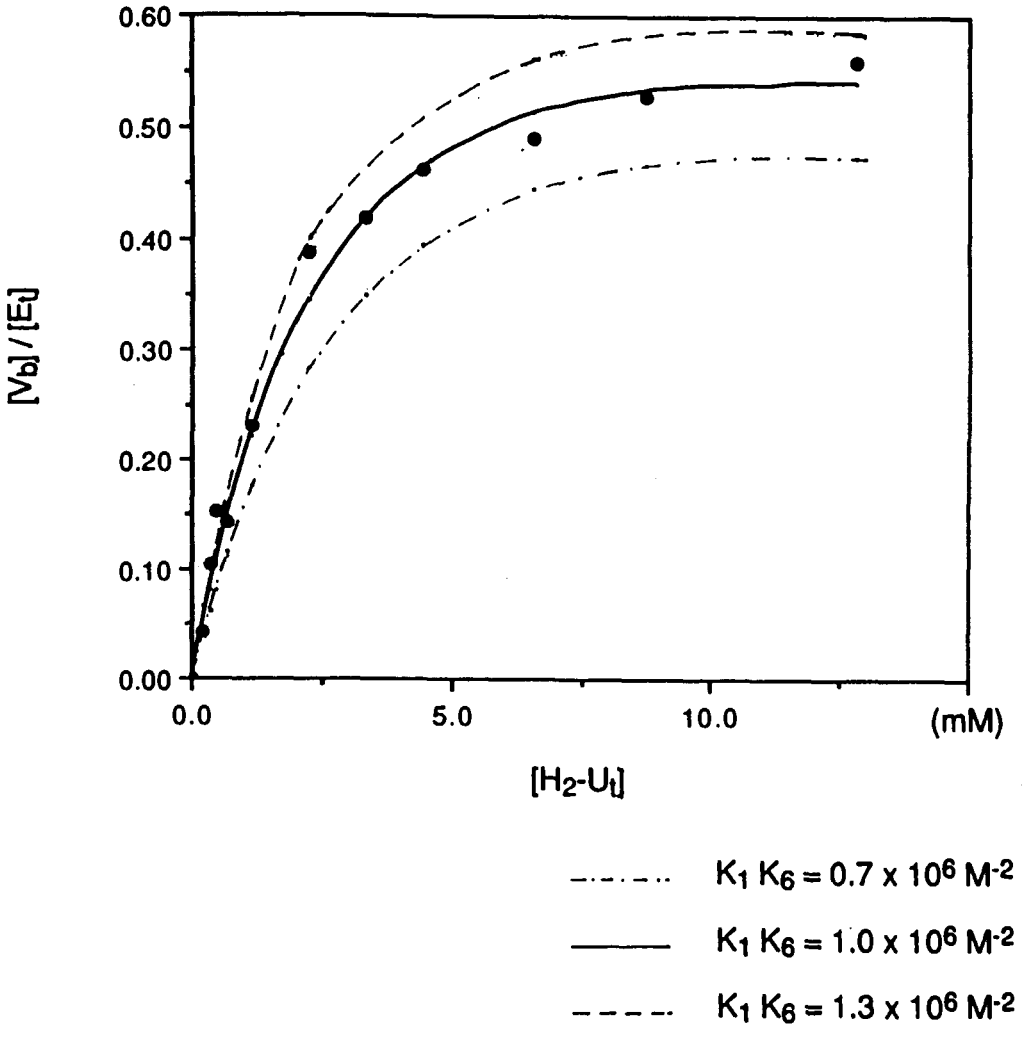

Fig. III.3.2

Plot of $[V_b]/[E_t]$ versus $[H_2\text{-}U_t]$: Determination of the value of the product of the equilibrium constants K_1K_6 (K_1 = formation constant of mononuclear (1:1) 5,6-dihydrouridine-vanadate complex, K_6 = binding constant of (1:1) 5,6-dihydrouridine-vanadate complex to RNase A). $K_1K_6 = (1.0 \pm 0.3) \times 10^6\ M^{-2}$. The best fit was obtained when K_5 ($1/K_{iH2\text{-}U}$) = $2.8 \times 10^1\ M^{-1}$. Conditions were 5.0 mM total vanadate and 0.9 mM total RNase A, pH 7.0.

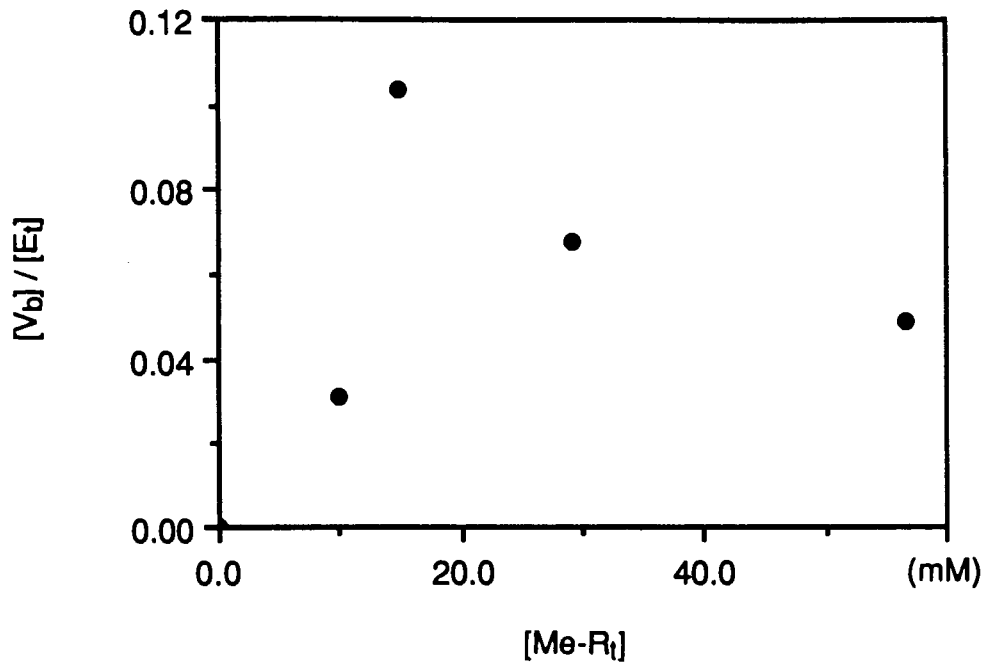

Fig. III.3.3

Plot of $[V_b]/[E_t]$ versus $[Me\text{-}R_t]$: Determination of the value of the product of the equilibrium constants K_1K_6 (K_1 = formation constant of mononuclear (1:1) methyl β-D-ribofuranoside-vanadate complex, K_6 = binding constant of (1:1) methyl β-D-ribofuranoside-vanadate complex to RNase A). The scatter in the experimental points indicates that K_1K_6 is not detectable. Conditions were 5.0 mM Tris buffer, 0.35 M KCl, 1 mM total vanadate and 0.7 mM total RNase A, pH 7.0.

$$2\ V_i + 2\ L \overset{K_3}{\rightleftharpoons} V_2L_2 \qquad K_3 = \frac{[V_2L_2]}{[V_i]^2[L]^2} \qquad (3)$$

$$E + L \overset{K_5}{\rightleftharpoons} E{\cdot}L \qquad K_5 = \frac{[E{\cdot}L]}{[E][L]} \qquad (25)$$

$$E + VL \overset{K_6}{\rightleftharpoons} E{\cdot}VL \qquad K_6 = \frac{[E{\cdot}VL]}{[E][VL]} \qquad (26)$$

$$E + V_i \overset{K_7}{\rightleftharpoons} E{\cdot}V_i \qquad K_7 = \frac{[E{\cdot}V_i]}{[E][V_i]} \qquad (27)$$

The inhibition constant K_{iVL} is the dissociation constant of VL from E·VL and so is equal to $1/K_6$.

By rearranging equations 1, 3, 4 and 25 and substituting into equation 22, the following rearranged expression is obtained:

$$[L]^2\ 2K_3\ [V_i]^2 + [L]\ (1 + K_1\ [V_i] + K_5\ [E] + K_1\ K_6\ [E]\ [V_i]) - L_t = 0 \qquad (28)$$

Similarly, by rearranging equations 23, 24, 1, 3, 25 and 26 and substituting into equation 21, and subsequent rearrangement, the following expression is obtained:

$$[V_i]^4\ 4K_4 + [V_i]^2\ 2(K_2 + K_3[L]^2) + [V_i](1 + K_1[L] + K_7[E] + K_1K_6[E][L]) - V_t = 0 \qquad (29)$$

Similar rearrangements and substitutions of equations 4, 25 and 26 into equation 20, will give the following equation:

$$[E] = \frac{[E_t]}{1+K_5[L]+K_1K_6[L][V_i]+K_7[V_i]} \qquad (30)$$

The fraction of total enzyme that is bound by vanadate (as a vanadate-ligand complex and/or vanadate alone) is:

$$\frac{[V_b]}{[E_t]} = \frac{[E{\cdot}VL]+[E{\cdot}V_i]}{[E_t]} \qquad (31)$$

By substituting the appropriate quantities into equation 31, the final equation obtained is:

$$\frac{[V_b]}{[E_t]} = \frac{[V_i](K_7+K_1K_6[L])}{1+K_5[L]+[V_i](K_7+K_1K_6[L])} \qquad (32)$$

A computer program was written to facilitate the numerical analysis for obtaining values of $[V_b]/[E_t]$ to construct a family of calculated curves. This program was not intended to be a statistical one, therefore the uncertainty reported for the value of K_1K_6 is estimated from the graph. Values for the equilibrium constants were: $K_2 = 470\ M^{-1}$, $K_4 = 6.3 \times 10^9\ M^{-3}$ (as mentioned earlier) and $K_7 = 0\ M^{-1}$. The K_2 (as defined by equation 24) value was obtained from ^{51}V NMR spectra of the same vanadate solutions used

to calculate K_4, in a similar fashion. A value of 0 for K_7 (as defined by equation 27) was assumed, since no binding of RNase A by vanadate was detected in any experiment. K_3 and K_5 will depend on the identity of the ligand. Values for $K_1 K_6$ were assumed in order to calculate the ratio $[V_b]/[E_t]$ as a function of [L], then varied until it was possible to assign a best fit value to K_1K_6. As can be seen in Fig. III.3.1, the best fit was obtained when $K_1 K_6$ was 6×10^6 M^{-2} and K_5 was 1.25×10^2 M^{-1} for the RNase A-uridine-vanadate system; in Fig. III.3.2, the best fit was obtained when $K_1 K_6$ was 1×10^6 M^{-2} and K_5 was 2.8×10^1 M^{-1} for the 5,6-dihydrouridine ligand. The other curves calculated from $K_1 K_6$ were used to obtain estimated upper and lower limits. An upper limit of 3.4 M^{-1} was given to K_1, so that a lower limit for K_6 (the binding constant of the vanadate-ligand complex to RNase A) could be calculated. In equation 32, $[V_i]$ value is obtained from equations 28-30. In order to determine the extent of the effect of K_1 on $[V_i]$, and therefore on the best fit value to K_1K_6 (6×10^6 M^{-2}), K_1 was varied from 0-3.4 M^{-1}. Values for $[V_i]$ were obtained at different K_1 values, and substituted into equation 32. K_1K_6 value was maintained constant. The shape and magnitude of the calculated curve did not change, indicating that the presence of free VL was not significant compared to the amount of VL bound to RNase A. This is an indication of the very small value of K_1, relative to the value of K_6.

Tables III.1, III.2 and III.3 show the distribution of the vanadate species among free and bound forms. Table III.4 shows the K_i's obtained from these equilibrium binding studies.

At the concentrations used in this study, it was found that no binding of the methyl β-D-ribofuranoside-vanadate complex to the enzyme was observed. An apparent disappearance of less than 5% of the total vanadate signals is seen at concentrations of methyl β-D-ribofuranoside from 15 mM to 60 mM. Since the uncertainty in the integration of the vanadium(V) signals can easily be 5%, it can be assumed that there is no binding of this vanadate-ligand complex to the enzyme. Another explanation of the small amount of V_b is non-specific binding of vanadate to RNase A, which cannot be detected in the cases of uridine-vanadate and 5,6-dihydrouridine-vanadate due to the tight binding of these complexes to RNase A. A lower limit for the dissociation constant ($K_{iMe\text{-}RV}$) was estimated by assuming that < 5% of the enzyme had complex bound to it when the concentration of the ligand was 60 mM. In view of these results, it is suggested that the role of the non-reacting portion of the substrate (in this case, the uracil group) is essential for the tight binding of the transition state analog to RNase A.

The K_i values determined for uridine-vanadate and 5,6-dihydrouridine-vanadate complexes are very similar (3×10^{-7} M and 2×10^{-6} M, respectively). This contrasts with the estimated lower limit for the K_i value of methyl β-D-ribofuranoside which is 2×10^{-4}

Table III.1

Distribution of vanadate among free and bound species with RNase A in the presence of uridine

$[U_t]$ (mM)	$[V_i]$ (mM)	$[V_{vis}]$ (mM)*	$[V_b]$ (mM)
0.0	0.356	1.00	0.00
0.2	0.347	0.90	0.10
0.3	0.314	0.76	0.24
0.4	0.321	0.74	0.26
0.6	0.293	0.63	0.37
1.0	0.266	0.51	0.49
2.0	0.231	0.37	0.63
4.0	0.172	0.26	0.74
6.9	0.136	0.24	0.76
7.9	0.118	0.20	0.80
12.0	0.093	0.22	0.78

* Vanadium atom concentration.
Concentration of total vanadium = 1 mM. Concentration of total RNase A = 0.9 mM. Conditions were 5.0 mM Tris buffer, 0.35 M KCl, pH 7.0. $[V_{vis}]$ = Visible vanadate species concentration. $[V_b]$ = RNase A bound vanadate concentration.

Table III.2

Distribution of vanadate among free and bound species with RNase A in the presence of 5,6-dihydrouridine

$[H_2\text{-}U_t]$ (mM)	$[V_i]$ (mM)	$[V_{vis}]$ (mM)*	$[V_b]$ (mM)
0.0	0.356	1.00	0.00
0.2	0.356	0.95	0.05
0.3	0.340	0.89	0.11
0.4	0.322	0.84	0.16
0.7	0.337	0.84	0.16
1.1	0.319	0.75	0.25
2.2	0.291	0.58	0.42
3.4	0.269	0.55	0.45
4.4	0.255	0.50	0.50
6.6	0.208	0.47	0.53
8.7	0.175	0.42	0.58
13.0	0.121	0.38	0.62

* Vanadium atom concentration.
Concentration of total vanadium = 1 mM. Concentration of total RNase A = 0.9 mM. Conditions were 5.0 mM Tris buffer, 0.35 M KCl, pH 7.0.

Table III.3

Distribution of vanadate among free and bound species with RNase A in the presence of methyl β-D-ribofuranoside

[Me-R_t] (mM)	[V_i] (mM)	[-523] (mM)*	[V_{vis}] (mM)*	[V_b][a] (mM)
0.0	0.375	0.000	1.00	0.00
10.0	0.304	0.337	0.97	0.02
15.0	0.245	0.498	0.91	0.08
30.0	0.153	0.728	0.92	0.05
60.0	0.081	0.822	0.91	0.04

* Vanadium atom concentration.
Concentration of total vanadium = 1 mM. Concentration of total RNase A = 0.7 mM. Conditions were 5.0 mM Tris buffer, 0.35 M KCl, pH 7.0.
[a] The small values for [V_b] indicate no significant binding of the methyl β-D-ribofuranoside. These numbers may be the result of experimental artifacts or non-specific binding of vanadate to RNase A.

Table III.4

Dissociation constants of various inhibitors of RNase A from NMR experiments

Inhibitor	$[L_t]$ (mM)	K_i [a] (mM)
Uridine-vanadate	0.0-12.0	$(3.3 \pm 0.6) \times 10^{-4}$ [b,c]
5,6-Dihydrouridine-vanadate	0.0-13.0	$(2.0 \pm 0.6) \times 10^{-3}$ [b,c]
Methyl β-D-ribofuranoside-vanadate	0.0-60.0	$> 2 \times 10^{-1}$ [b]

[a] K_i = dissociation constant of the ligand-vanadate-enzyme complex ($K_i = 1/K_6$).
[b] K_i's were calculated assuming a value for $K_1 = [VL]/([V_i]\,[L]) = 2.0\ M^{-1}$.
Conditions of these experiments were 5.0 mM Tris buffer, 0.35 M KCl, pH 7.0 and room temperature. The total vanadate concentration was approximately 1.0 mM. $[L_t]$ = total ligand concentration, $[V_t]$ = total vanadate concentration.
[c] Errors are estimated from the graphs in Fig. III.3.1 and III.3.2.

M. This indicates that if there is binding of this complex, it is at least 100 times less tight than for the complex of vanadate with dihydrouridine and at least a factor of 1,000 from that of the uridine-vanadate complex. It seems apparent that at least a pyrimidine residue is required in order for significant binding of the vanadate complex to occur. Although the uridine and 5,6-dihydrouridine bind at a subsite which is distant from the centre of reaction, it seems apparent that a conformational change is occurring upon binding of these vanadate-nucleoside complexes. Another explanation would be that the binding is tighter when the ligand of the vanadate complex is a larger molecule, so that it can occupy the whole subsite. However, previous X-ray and circular dichroism studies have shown that a conformational change occurs upon binding of inhibitors to RNase A, as described in Chapter IV.

The results described above are consistent with two possible catalytic mechanisms for RNase A: An induced-fit mechanism or an induced destabilization mechanism. The induced-fit mechanism describes a substrate-induced conformational change of the enzyme that brings catalytic groups into contact with reactive groups on the substrate, but it does not include cases in which the conformational change causes strain, distortion, or any other kind of destabilization of the enzyme-substrate complex. The induced destabilization mechanism involves strain or distortion of the bound substrate, mediated by a conformational change of the enzyme.

During the ligand titration experiments, it was found that after addition of uridine and 5,6-dihydrouridine, the pH of the enzyme solution increased. This observation is similar to that reported for phosphate-containing compounds (44), and it indicated that protons are taken up during the association of ligands with RNase at pH above 5.5.

III.2. Kinetic Studies: Hydrolysis of Uridine 2',3'-Cyclic Monophosphate Catalyzed by RNase A

III.2.1. Experimental procedure

III.2.1.1. Preparation of vanadate, ligands, substrate and enzyme stock solutions

Stock solutions of 1.0 mM sodium vanadate were prepared by dilution of a 100 mM solution of vanadate. This dilution was made in 5.0 mM Tris buffer and the pH was adjusted to 7.0 with small aliquots of 0.1 N NaOH before bringing up to the final volume.

Stock solutions of uridine, 5,6-dihydrouridine and methyl β-D-ribofuranoside were prepared as described in Section II.1.1.2.

A solution of the substrate, uridine 2',3'-cyclic monophosphate, in 5.0 mM Tris buffer, pH 7.0, was prepared fresh on the same day, prior to a series of kinetic runs, and kept on ice. Concentrations of uridine and uridine 2',3'-cyclic monophosphate were determined by UV spectrophotometry (E_{260} = 9.9 $mM^{-1}\,cm^{-1}$ for uridine and E_{258} = 9.57 $mM^{-1}\,cm^{-1}$ for uridine 2',3'-cyclic monophosphate).

Two enzyme stock solutions were prepared by dissolving the lyophilized powder in 5.0 mM Tris buffer and the pH was adjusted to 7.0 with very small aliquots of 0.05 N NaOH with gentle stirring. The concentrations of the stock solutions of RNase A were

1.59 mg/ml and 1.46 mg/ml determined by UV spectrophotometry ($E_{280}^{1\%} = 7.3$).

III.2.1.2. Instrumentation

Reaction rates were obtained by following the change in absorbance at 286 nm on a Hewlett Packard 8452A diode array spectrophotometer.

The signal averaging time was 10 s, the scanning interval was 35 s and the reaction rates were followed for 10 min.

III.2.1.3. Rate measurement

3 ml UV cells containing cylindrical magnetic stir bars were used for the kinetic runs. Samples were prepared by mixing appropriate amounts of the stock solutions to obtain the desired final concentrations. Conditions of the assay were 5.0 mM Tris buffer, 0.35 M KCl, 14-16 μg/ml RNase A at pH 7.0 and 25 °C.

The rate of hydrolysis of uridine 2',3'-cyclic monophosphate was monitored at 286 nm. The absorbance is based on the difference in extinction coefficient of uridine 2',3'-cyclic monophosphate and uridine 3'-monophosphate, $\Delta E_{286} = 600\ M^{-1}cm^{-1}$ (45), which results mainly from the difference in the number of charges on the molecules as shown in scheme III.4.

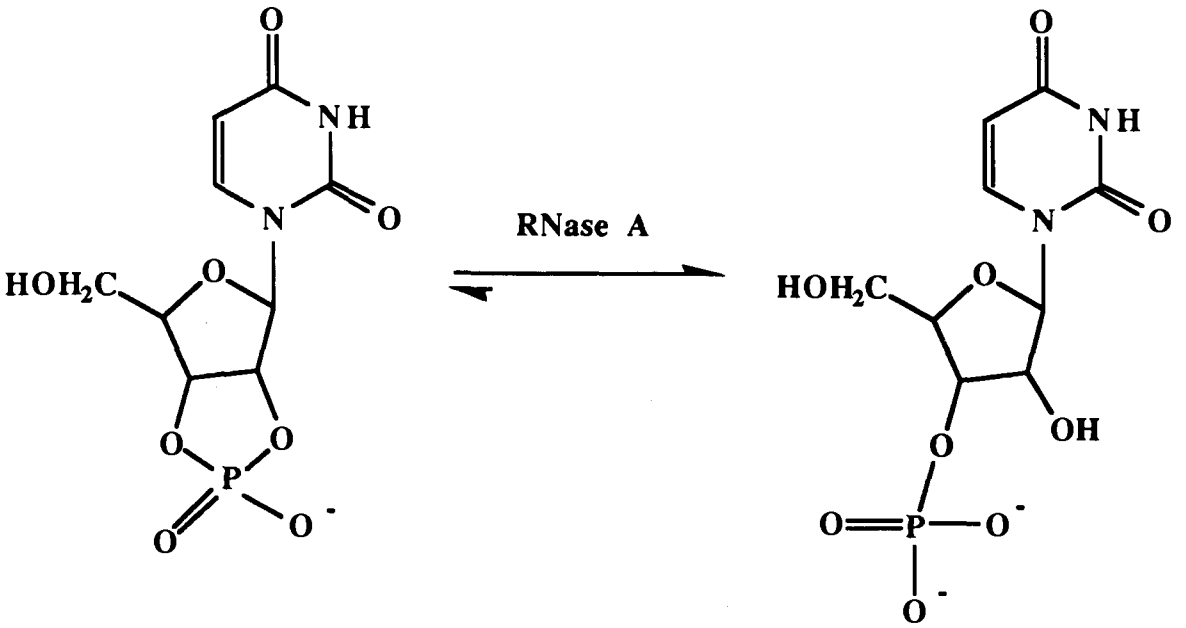

(III.4)

The reactions were started by addition of 20 µl of RNase A to 2.0 ml reaction mixtures (final concentration of enzyme was 14-16 µg/mL), and the rate measurements were started 1.5 min after the addition of the enzyme. The measurement time was 3 min. In most of the cases, the changes in the absorbance rates were linear with time indicating that product (uridine 3'-monophosphate) inhibition was insignificant. The rates were proportional to enzyme concentration.

III.2.2. Results and discussion: Effect of uridine, 5,6-dihydrouridine and methyl β-D-ribofuranoside on the rate of hydrolysis of uridine 2',3'-cyclic monophosphate catalyzed by RNase A

The classical Michaelis-Menten equation was inverted to give a linear equation,

$$\frac{1}{v} = \frac{1}{V_{max}} + \frac{K_m}{V_{max}[S]} \qquad (33)$$

where v = reaction rate, V_{max} = maximal reaction rate, K_m = Michaelis constant or apparent dissociation constant of U-2',3'-P, and [S] = U-2',3'-P concentration, so that the kinetic data could be analyzed in an easier way. In the case of inhibition, the appropriate inhibition terms were added to the Michaelis-Menten equation and inverted. For inhibition by uridine and 5,6-dihydrouridine, the equation was

$$\frac{1}{v} = \frac{K_m}{V_{max}}\left(1 + \frac{[L]}{K_{iL}}\right)\frac{1}{[S]} + \frac{1}{V_{max}} \qquad (34)$$

where K_{iL} = inhibition constant of the ligand. In the cases of inhibition by uridine-vanadate and 5,6-dihydrouridine-vanadate complexes, the corresponding equation was

$$\frac{1}{v} = \frac{K_m}{V_{max}}\left(1 + \frac{[L]}{K_{iL}} + \frac{K_1[L][V_i]}{K_{iVL}}\right)\frac{1}{[S]} + \frac{1}{V_{max}} \qquad (35)$$

where K_{iVL} = inhibition constant of the vanadate-ligand complex. In equation 35, the term [VL] was substituted by K_1 [L] [V_i].

At 39.6 mM 5,6-dihydrouridine and 0.1 mM vanadate, a significant fraction of the total vanadate is in the form V_2L_2. In order to calculate the concentration of free vanadate, the following conservation equation was considered:

$$[V_t] = 2[V_2L_2] + [VL] + [V_i] + [E{\cdot}VL] \quad (36)$$

At these concentrations, since [VL] represents about 2% and [E·VL] is much less than 1% of the total vanadate concentration, equation 36 can be approximated to

$$[V_t] = 2[V_2L_2] + [V_i] \quad (37)$$

$[V_2L_2]$ is defined by the following expression

$$K_3 = \frac{[V_2L_2]}{[V_i]^2[L]^2} \quad (3)$$

Rearranging equation 3 and substituting into equation 37, yields equation 38,

$$2K_3[L]^2[V_i]^2 + [V_i] - [V_t] = 0 \quad (38)$$

which is a quadratic equation expressed in terms of $[V_i]$. Solving equation 38 for $[V_i]$, gives the values to be used in analyzing the data in terms of equation 35.

Double reciprocal plots are shown in Fig. III.4 and III.5. All curves have a common y intercept (which represents $1/V_{max}$) indicating that the inhibitors are competitive with the substrate. The x intercept represents $1/K_{mapp}$ of the substrate (K_{mapp} = apparent K_m). The K_{mapp} value in the absence of inhibitor is 4.3 mM. Rates were normalized to 1 mg/ml of enzyme. The values of K_i ($K_{iUV} = 3 \times 10^{-4}$ mM and $K_{iH2\text{-}UV} = 8 \times 10^{-4}$ mM) were obtained from the slopes of the plots and the value of K_m/V_{max} which was determined in the absence of inhibitor.

A site (p_o site) may exist for the binding of the 5'-phosphate of compounds such as pUp (46). In order to determine whether the inhibition is due to a (1:1) or a (1:2) uridine-vanadate complex, the effect of different concentrations of vanadate on the rate of hydrolysis of a fixed concentration of uridine 2',3'-cyclic monophosphate was studied. Analysis of these data requires a rearrangement of equation 35, which gives

$$\frac{1}{v} = \frac{K_m K_1 [L]}{V_{max} K_{iVL} [S]} \cdot [V_i] + \frac{K_m}{V_{max}[S]} \left(1 + \frac{[L]}{K_{iL}}\right) + \frac{1}{V_{max}} \qquad (39)$$

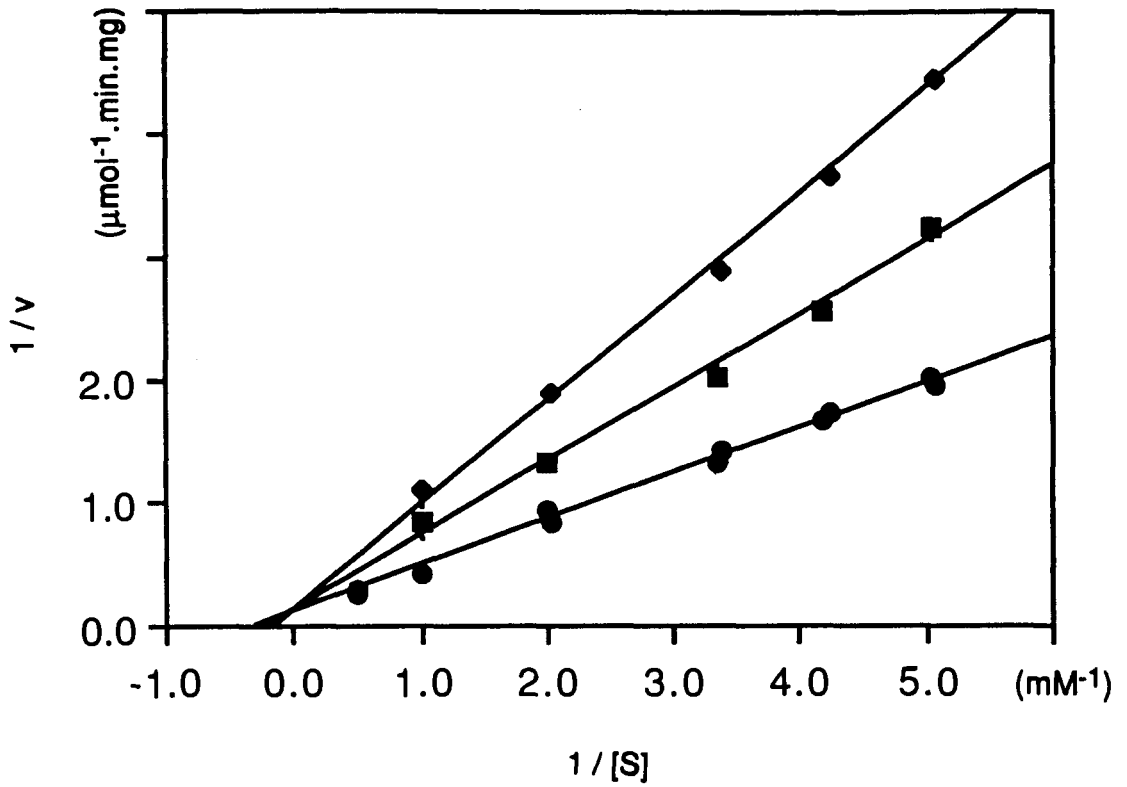

Fig. III.4

Lineweaver-Burk plot of the rate of hydrolysis of uridine 2',3'-cyclic monophosphate catalyzed by RNase A in the presence of uridine and/or vanadate. Inhibitors: None (•); 1 mM U_t (■); 1 mM U_t + 0.1 mM V_t (◆). All velocities have been normalized to the same concentration of enzyme. Conditions: 5.0 mM Tris buffer, 0.35 M KCl, at 25 °C and pH 7.0. Concentration of enzyme was 14-16 µg/mL. The experimental points represent the average of at least two independent determinations.

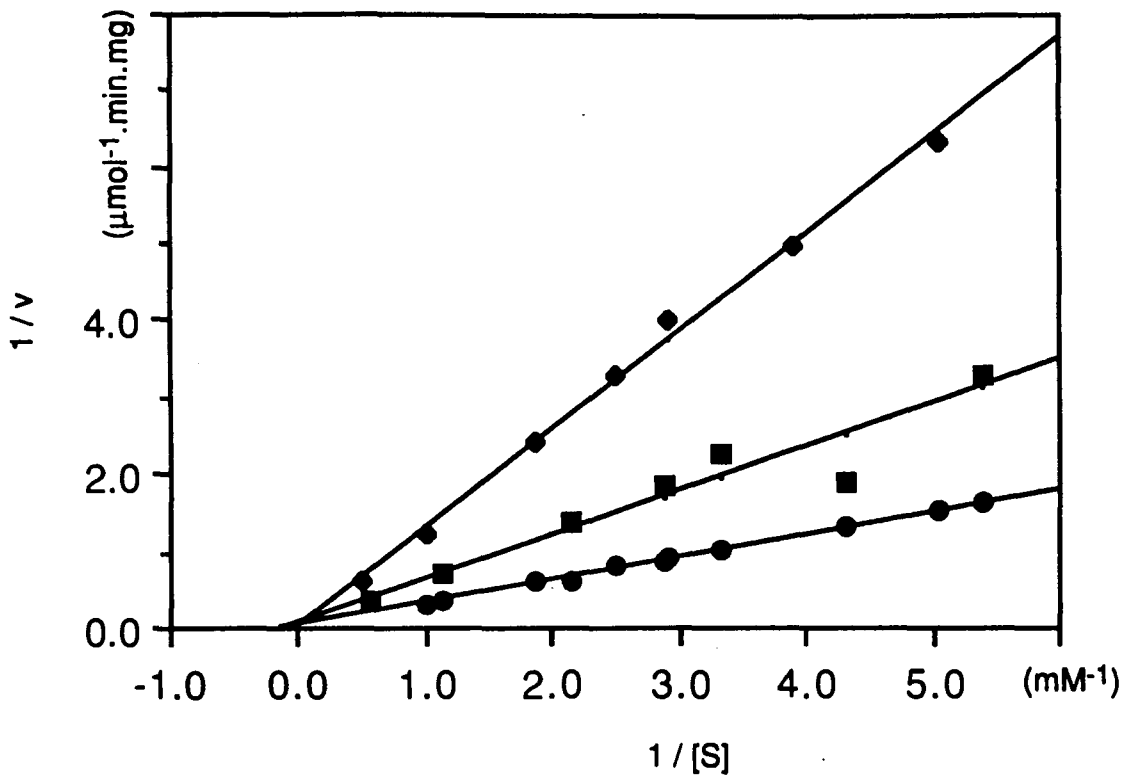

Fig. III.5

Lineweaver-Burk plot of the rate of hydrolysis of uridine 2',3'-cyclic monophosphate catalyzed by RNase A in the presence of 5,6-dihydrouridine and/or vanadate. Inhibitors: None (•); 39.6 mM H_2-U_t (■); 39.6 mM H_2-U_t + 0.1 mM V_t (◆). All velocities have been normalized to the same concentration of enzyme. Conditions: 5.0 mM Tris buffer, 0.35 M KCl, at 25 °C and pH 7.0. Concentration of enzyme was 14-16 μg/mL.

Since [S] and [L] are in large excess relative to the concentration of enzyme and the concentration of V_2L_2 is less than 1% of the concentration of total vanadate, under the conditions shown in Fig. III.6, [S] and [L] can be approximated to $[S_t]$ and $[L_t]$ which were kept constant, so this equation predicts a straight line. If the inhibition is due to a (1:1) uridine-vanadate complex, a linear plot should be obtained. If the inhibition is due to a (1:2) uridine-vanadate complex, a linear plot would be obtained when 1/v is plotted against $[V_i]^2$. Fig. III.6a and III.6b show the plots according to each analysis. Straight lines are obtained in both cases, indicating that it is not possible to distinguish which is the inhibitory species, in the concentration range of uridine and vanadate studied. However, the ^{51}V NMR experiments on RNase A and neutron diffraction studies show that the binding species is a (1:1) uridine-vanadate complex.

At a concentration of 0.1 mM, vanadate does not observably inhibit RNase A. Inhibition constants for vanadate complexes were calculated from the slopes shown in Fig. III.4 and III.5, and reported in Table III.5. Comparison of the different K_i values indicates that 5,6-dihydrouridine binds with a lower affinity than uridine by about a factor of 5. Upon addition of vanadate to each inhibitor, K_i's for both inhibitors were greatly decreased, indicating inhibition by a vanadate-ligand complex. K_i for uridine-vanadate complex was at least 10^3 times smaller than K_i for uridine; and K_i for 5,6 dihydrouridine-vanadate complex was at least 10^3

times smaller, compared to K_i for 5,6-dihydrouridine. It is obvious that the binding of both nucleosides is enhanced upon addition of vanadate. The K_i values for both vanadate complexes are much smaller than the K_{mapp} value (4.3 mM) for the substrate, indicating that these vanadate complexes are transition state analogs.

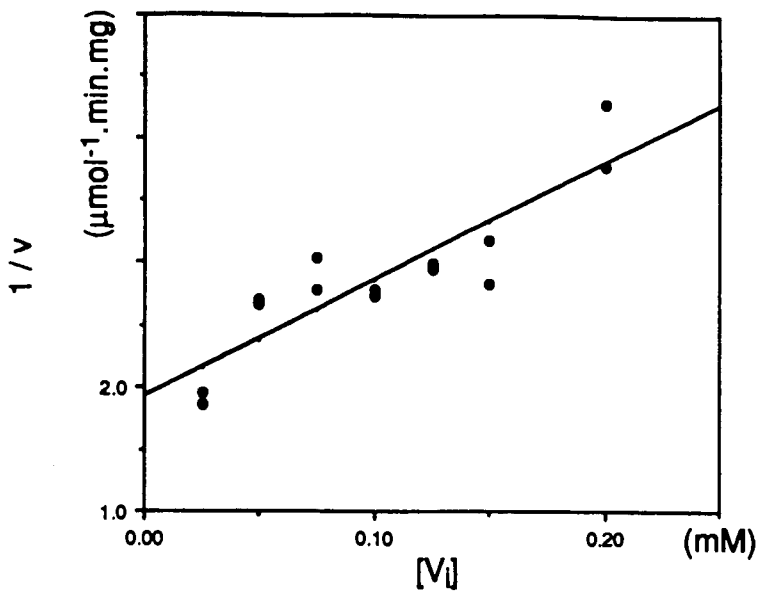

Fig. III.6a

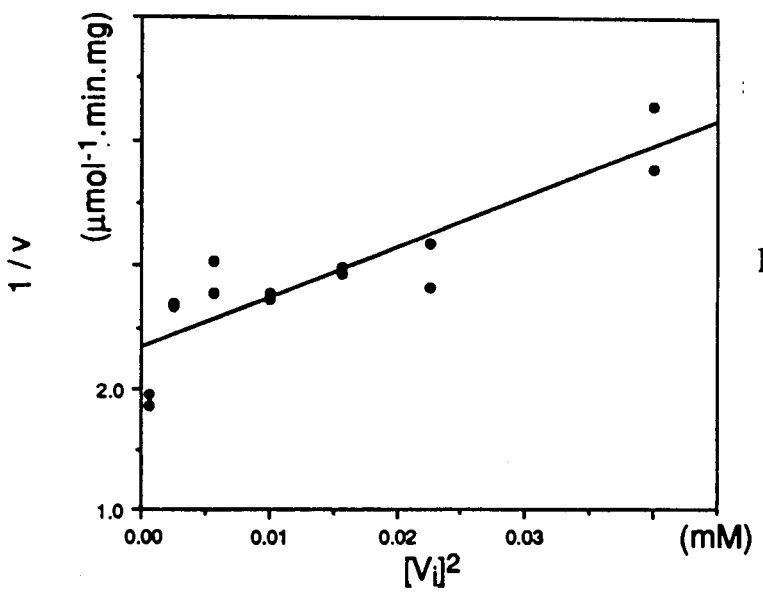

Fig. III.6b

Dependence of the inhibition of hydrolysis of uridine 2',3'-cyclic monophosphate catalyzed by RNase A on the concentration of vanadate, in the presence of 0.99 mM uridine. Conditions: 5.0 mM Tris buffer, 0.35 M KCl, at 25 °C and pH 7.0. Concentration of enzyme was 14-16 μg/mL.

Table III.5

Dissociation constants of various inhibitors of RNase A determined from kinetic experiments

Inhibitor	$[L_t]$ (mM)	$[V_t]$ (mM)	K_i (mM)
Uridine 2',3'-cyclic monophosphate			4.3 ± 1.3 [a]
Uridine	0.99		1.7 ± 0.1 [b]
5,6-Dihydrouridine	39.6		42 ± 6 [b]
Uridine-vanadate	0.99	0.1	(3.0 ± 0.2) x 10^{-4} [b,c]
5,6-Dihydrouridine-vanadate	39.6	0.1	(7.6 ± 0.8) x 10^{-4} [b,c]

[a] K_{mapp} value for the substrate. The error is the standard deviation obtained from two K_{mapp} determinations.
[b] Errors were calculated from a least-squares analysis on the double reciprocal plots.
[c] K_i's were calculated assuming a value for $K_1 = [VL]/([V_i]\,[L]) = 2.0\ M^{-1}$.
Conditions of these experiments were 5.0 mM Tris buffer, 0.35 M KCl, pH 7.0 and 25 °C.

III.3. PH Studies: An Informative Approach to the Investigation of Ligand Binding to RNase A

Kinetic studies using competitive inhibitors are very useful for investigating enzymatic reaction mechanisms, however, ligand binding studies can provide additional information about the nature of the binding site. Complex formation between an enzyme and a substrate or a competitive inhibitor may depend on several factors, such as ionic strength, pH, temperature, etc. Studies of some of these factors may provide a further insight into the active site.

In previous experiments, significant pH shifts were observed when adding a nucleoside into an enzyme solution containing vanadate. From these findings, it was decided to investigate in some detail this pH dependence of the enzyme-inhibitor complex formation.

III.3.1. Experimental procedure

III.3.1.1. Preparation of samples and solutions

Solutions of 0.01 N HCl and 0.01 N NaOH were prepared in 0.09 M KCl. Solutions of RNase A were prepared by dissolving appropriate quantities of the lyophilized powder in unbuffered 0.10 M KCl to give a final concentration of 0.21 - 0.25 mM enzyme. A solution of 0.05 N NaOH was used to adjust the pH of the enzyme solutions to approximately 6, before addition of vanadate (1 mM).

The pH was then adjusted to the desired value. Similarly, a stock solution of uridine (0.2 M) was prepared by dissolving appropriate amounts of the powder in unbuffered 0.10 M KCl, and the pH was adjusted to the same pH as that of the enzyme solution. Concentrations of RNase A and uridine were determined by UV spectrophotometry as described in Section III.2.1.1.

III.3.1.2. Instrumentation

The pH measurements were made on an Accumet pH meter 915 from Fisher Scientific, with a glass combination electrode with calomel reference (model 13-620-270). The pH meter was calibrated at pH 4.00 and 7.00 using freshly opened reference buffer solutions, prior to each titration. A Hamilton syringe was used to deliver the amount of HCl or NaOH required to adjust the pH of the samples.

III.3.1.3. H^+ uptake or release measurement

Enzyme samples of 1.0 ml containing small magnetic stir bars were used. After measuring the previously adjusted pH, an aliquot of the inhibitor stock solution was added, and the pH increased immediately. In order to quantitate the amount of H^+ taken up, the volume of 0.01 N HCl in 0.09 M KCl required to adjust the pH back to its initial value was measured. A 10.0 µL Hamilton syringe was used to measure and deliver small aliquots of the HCl to the

sample, to reestablish the initial pH. The ligand titration was carried on in this way until the pH remained constant. A blank titration was performed, using a 0.10 M KCl solution without enzyme, with pH adjusted to the desired value. This would account for possible changes in pH due to breakdown of vanadate oligomers upon dilution.

III.3.2. Results and discussion: Hydrogen ion requirements for the formation of a uridine-vanadate-RNase A complex

During the course of preliminary experiments concerning the binding of the uridine-vanadate complex to RNase A it was observed that one of the results of mixing the various stock solutions, all prepared at the same pH, was a change in pH in the resultant product solution. An effort was then made to measure this effect more quantitatively.

A plot of the number of moles of H^+ taken up per mole of RNase A in the presence of 0.99 mM vanadate, as a function of the total concentration of uridine is seen in Fig. III.7. It can be seen in this figure that the ratio of H^+ taken up per mole of enzyme increases when the total uridine concentration increases, at a fixed total vanadate concentration. Since no change in the pH is caused by addition of nucleosides to RNase A (44) and no binding of vanadate was detected in the ^{51}V NMR studies, it is suggested that H^+ uptake is due to the association of the uridine-vanadate complex with RNase A.

Possible changes in pH associated with the effect of the free uridine-vanadate complex on the equilibria between the free vanadate species are already taken into account. This was done by performing a blank titration, i.e., a titration of the uridine-vanadate system in the absence of RNase A. Thus, the pH changes observed in these experiments are ascribed entirely to the formation of a uridine-vanadate-RNase A complex. When the ligand titration was performed at pH 6.50, the ratio of H^+ taken up per mole of enzyme was 0.27, at saturation. If the free enzyme exists in different protonation states, when the pH is raised, the equilibria between the free enzyme species will be shifted towards a more deprotonated state of the enzyme, $H \cdot E^+$. This behaviour is represented in Scheme III.8 which considers the possible different equilibria present in the system.

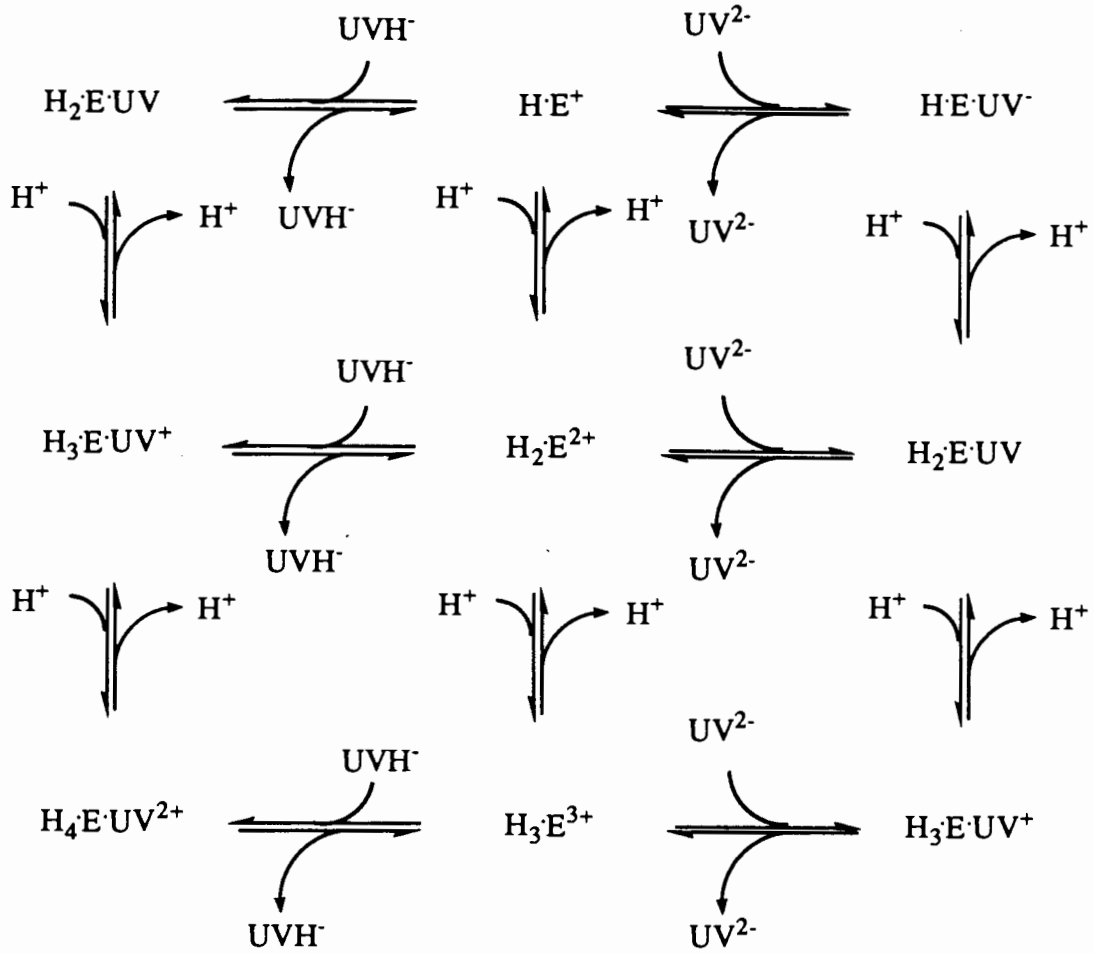

(III.8)

The pK_a's of His-12 and His-119 in the free RNase A are 5.8 and 6.2 (31,32), it is likely that at least one deprotonated histidine will react with a proton to facilitate the binding of the uridine-vanadate complex. At a higher pH, more H^+ will be taken up by the enzyme species in order to restore $[H_3 \cdot E^{3+}]$ and $[H_3 \cdot E \cdot UV^+]$ at equilibrium. This can be seen in Fig. III.7, when the pH is 6.90, a ratio of $[H^+_b]$ /$[E_t]$ of 0.60 is obtained under saturating conditions. At the pH range studied

(6.50 - 6.90), the equilibrium between the monoanionic and dianionic uridine-vanadate complexes is very sensitive to pH, since the pK_a of this complex is approximately 6.7 (4,5). However, consideration has to be taken on the effect of this inhibitor on the pK_a's of the amino acid residues in the active site. It is expected that these pK_a values will increase upon binding of a negatively charged ligand into the active site.

Neutron diffraction studies (27) have shown that the uridine-vanadate complex is bound to the enzyme by hydrogen bonds to both His-12 and 119 as well as Lys-41, i.e., three H^+ ions are required to form this enzyme-inhibitor complex. Lys-41 is likely to be fully protonated because it has a high pK_a. A simple H^+ transfer between the vanadate moiety and the amino acid residues at the active site might be involved as the $H_3 \cdot E \cdot UV^+$ complex is formed. The results obtained from these pH studies showed a net H^+ uptake upon addition of ligand. This would result in a net increase in pH, which is consistent with the results from neutron diffraction studies.

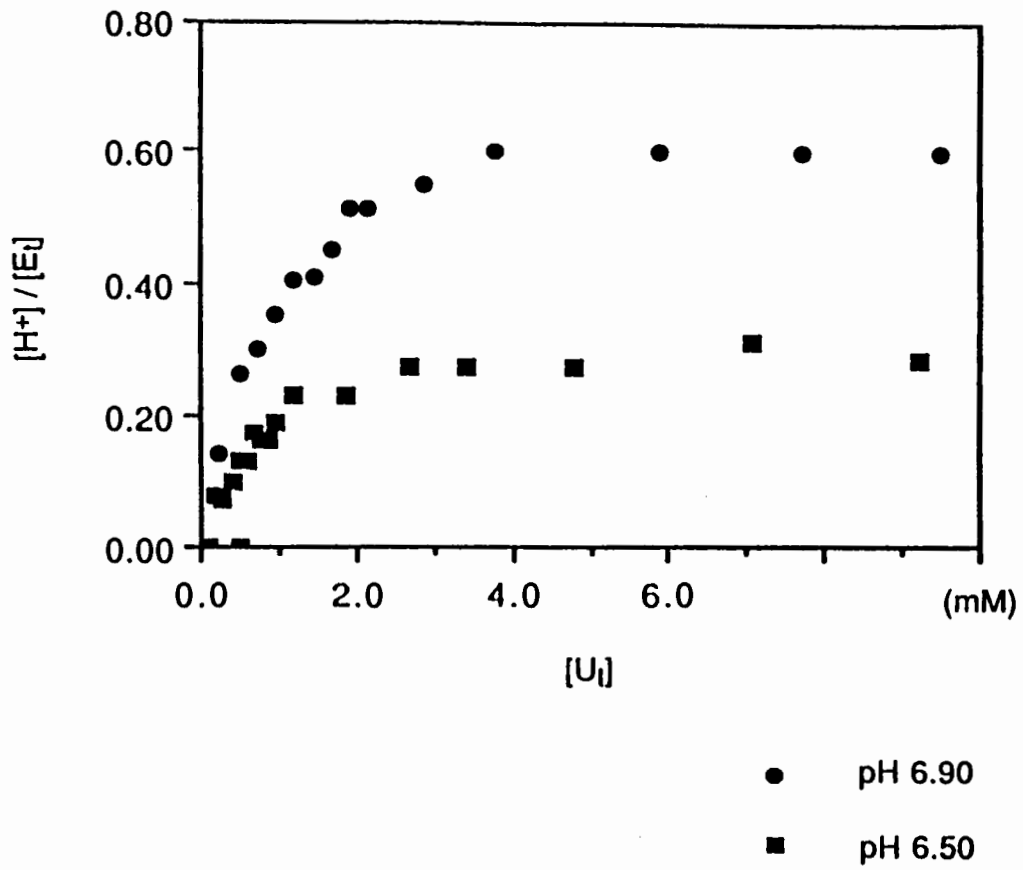

Fig. III.7

Dependence of the concentration of H^+ taken up in a uridine-vanadate-RNase A system as a function of the concentration of total uridine. Conditions were 0.10 M ionic strength with added KCl, 1 mM total vanadate. Protein concentration = 0.21-0.25 mM.

Chapter IV
Discussion

In an effort to study how enzymes catalyze a reaction, it would be desirable to study the transition state of the reaction. Unfortunately, the transition state itself has a very short lifetime to permit its study, but an indirect approach may provide a partial solution to this problem: Namely the use of transition state analogs. A transition state analog for an enzyme is a stable compound that resembles in structure the substrate portion of the transition state of the enzymatic reaction (47). A transition state analog is an ideal inhibitor, since it resembles in its binding properties the activated substrate moiety of the transition state complex and it should be bound much more tightly to the enzyme than the substrate. From a group of reversibly bound substrate analogs, an enzyme should thus select for tight binding those which most closely resemble the transition state structure, not the substrate itself. The use of transition state analogs for kinetic and equilibrium studies can thus provide support for an enzyme mechanism, and they are a practical tool for the design of metabolic inhibitors.

Vanadate complexes (pentacoordinate, trigonal bipyramidal) are potent transition state analogs for some phosphoryl-transferring enzymes. The enzyme RNase A, which catalyzes the hydrolysis of the 2'-O-P bond of pyrimidine 2',3'-cyclic

monophosphates, is potently inhibited by uridine 2',3'-cyclic monovanadate and 5,6-dihydrouridine 2',3'-cyclic monovanadate, which are transition state analogs. The association constant for the binding of these compounds to the enzyme at pH 7.0 is at least 10^3 times larger than the kinetically estimated association constant for the uridine 2',3'-cyclic monophosphate. Since vanadate anions are known to form stable pentacoordinate trigonal bipyramidal complexes with ribose-containing ligands, the structure for the complex between the enzyme and uridine 2',3'-cyclic monovanadate is one in which the amine group of Lys-41 and the imidazole rings of His-12 and His-119 form hydrogen bonds with the oxygens of vanadium(V). This structure is similar to the trigonal bipyramidal transition state that is proposed for the hydrolysis of pyrimidine 2',3'-cyclic monophosphates catalyzed by RNase A (ref. 9, 11).

The complex formed between uridine and vanadate inhibited RNase A with a binding constant (K_6) of 3×10^6 M^{-1}. When a 5,6-dihydrouridine-vanadate complex was used instead of the uridine-vanadate complex, K_6 was approximately 5×10^5 M^{-1}. A synergistic interaction is suggested between the pyrimidine and the vanadate groups. The degree of synergism between the 5,6-dihydrouridine and the vanadate groups was diminished, indicating a relatively important role for the amino acid residues Thr-45, Phe-120 and Val-43 which interact with the base. When a methyl β-D-ribofuranoside-vanadate complex was used in the inhibition studies,

it was found that no binding to RNase A was observed, at the concentration range studied. Also, vanadate itself does not bind to RNase A, at the concentrations used. A lower limit for K_i of vanadate is estimated to be 1×10^{-3} M, that is, $K_6 < 1 \times 10^3$ M^{-1}. The substitution of a pyrimidyl group by a β-methoxy group decreased the affinity of the enzyme for the vanadate group by at least 500-fold. This requirement for a uridine or 5,6-dihydrouridine group suggests that the minimal structure necessary to stimulate the binding of the vanadate appears to be that of a pyrimidine group.

To explain the observed effects, it is suggested that there are two interconvertible conformations of RNase A which differ in their affinity toward these vanadate-complex inhibitors. The low affinity or inactive form (E) is complementary to the substrate, while the high affinity or active form (E^*) has a structure complementary to that of the transition state (see Fig. IV.1). In the absence of either group (the pyrimidyl or the ribose-vanadate group), the enzyme is predominantly in the low affinity form. The binding of either group by itself is consequently unfavorable. However, in the presence of both groups, the equilibrium between the RNase A species is shifted to the high affinity form. These synergistic effects exerted by the ribose-vanadate and the pyrimidyl groups upon binding to E are explained graphically in Scheme IV.1 and Fig. IV.1. Either domain or subsite, once it is occupied by its corresponding group, causes a change in state of both domains so that both groups of the ligand are

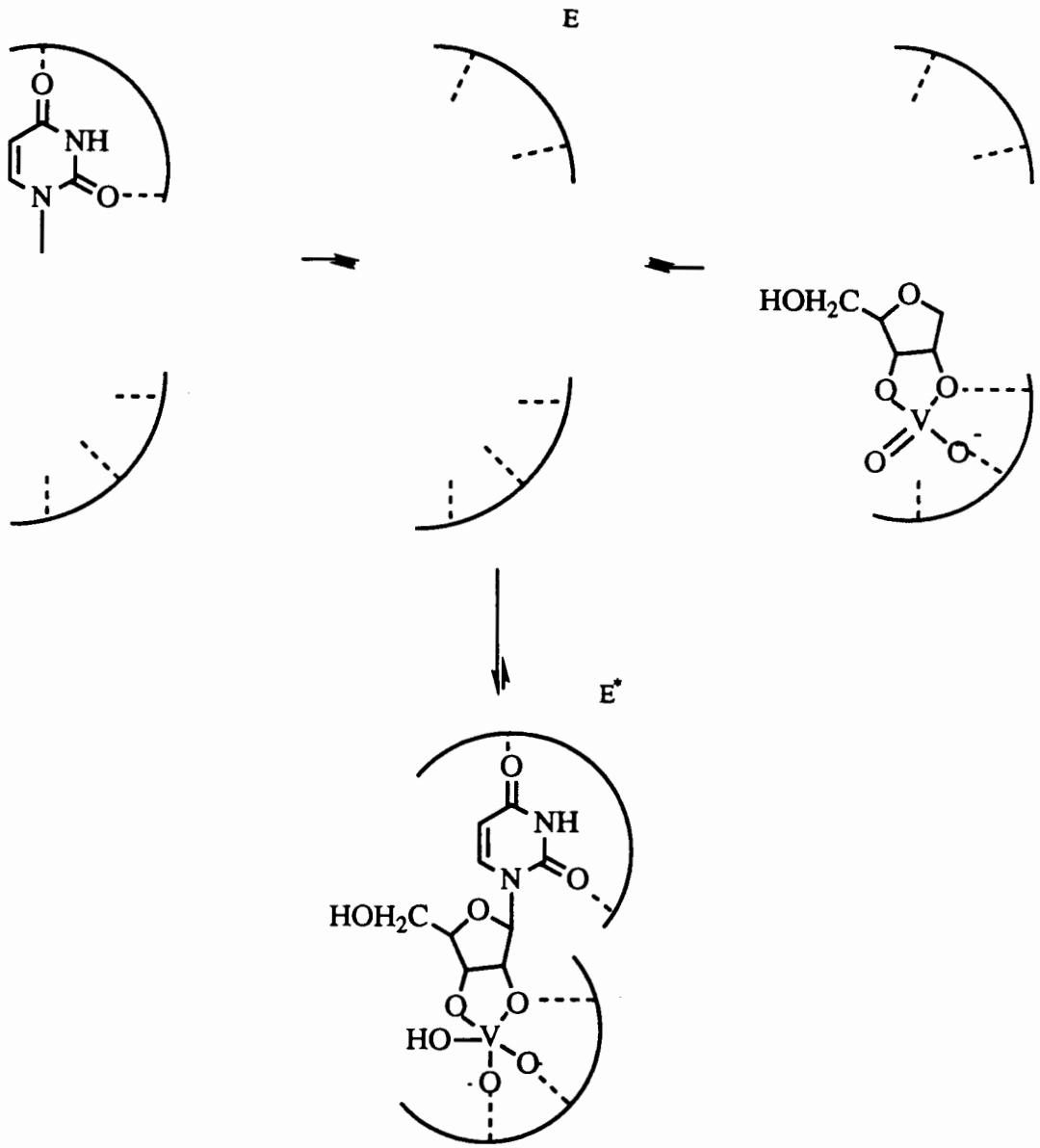

Fig. IV.1

Synergistic effects of ribose-vanadate and pyrimidyl groups upon binding to RNase A

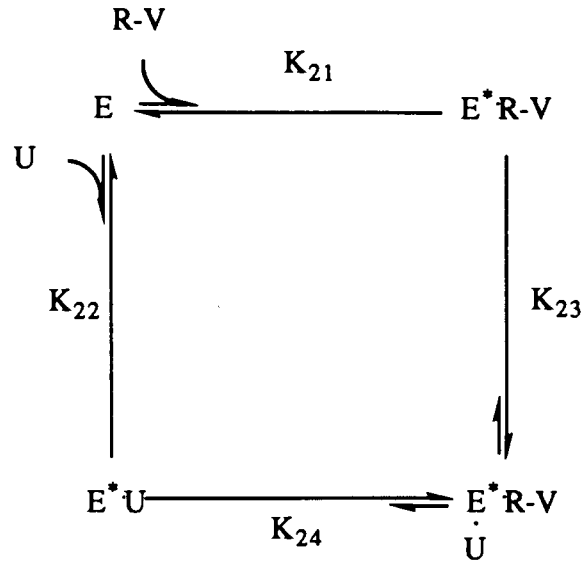

R-V = ribose-vanadate complex

U = uracil ligand

E = inactive enzyme conformation

E^* = active enzyme conformation

(IV.1)

accomodated better, and therefore, an energetically favorable interaction can occur.

The synergism observed in RNase A is also observed in phosphoglucomutase: The binding of both sugar and phosphate increases the rate of phosphate transfer to ROH even when (a) ROH is water or (b) the sugar and phosphate are not connected by a covalent bond. These results show that binding at the phosphate site

and the sugar site, independently or concurrently, leads to large decreases in the free energy of activation (48).

Since vanadate can exist in solution as a tetrahedral or as a pentacoordinate species when complexed to a ribose-containing ligand, it is possible that both species bind to the enzyme, the tetrahedral species will bind to E and the pentacoordinate species will bind to E*, as shown in Scheme IV.2. The pentacoordinate

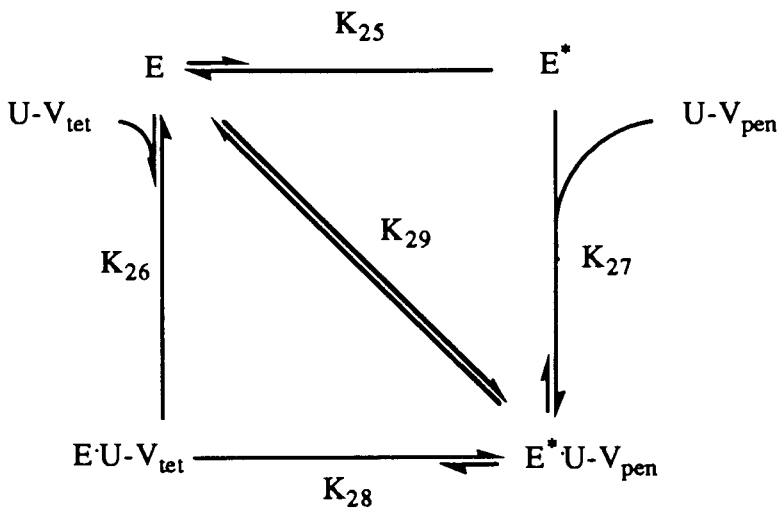

$U\text{-}V_{tet}$ = tetrahedral uridine-vanadate complex

$U\text{-}V_{pen}$ = pentacoordinate uridine-vanadate complex

E = inactive enzyme conformation

E* = active enzyme conformation

(IV.2)

pyrimidine-vanadate complex should have an intrinsic tight binding to E^*, however, this very tight binding overall is not seen because the equilibrium K_{25} is very unfavorable. Thus the observed binding energy represents the algebraic sum of the favorable binding of inhibitor plus the unfavorable transition from E to E^*.

When proposing the mechanism of action for the hydrolysis of U-2',3'-P by RNase A, only the tetrahedral phosphate species will bind to the enzyme (the E conformation) since the pentacoordinate phosphate species is too unstable to exist free in solution. The proposed mechanism of action is represented by Scheme IV.3. As can be seen, the tetrahedral phosphate substrate (S) binds to the enzyme conformation E to possibly form an E·S complex and this leads to the formation of the transition state E^*·S'.

The induced-fit mechanism, as proposed by Koshland (49) states that the catalytic groups at the active site of the free enzyme are not in optimal positions in which they can exert effective catalytic activity. According to this mechanism, a substrate must have the necessary structural features to force a conformational change of the enzyme to the active form, and, therefore, to undergo a reaction. This mechanism for RNase A is supported by the direct ^{51}V NMR binding studies and the kinetic inhibition studies in this work using vanadate complexes, in which methyl β-D-ribofuranoside-vanadate complex is not an inhibitor (no binding or inhibition detected at the concentration range studied).

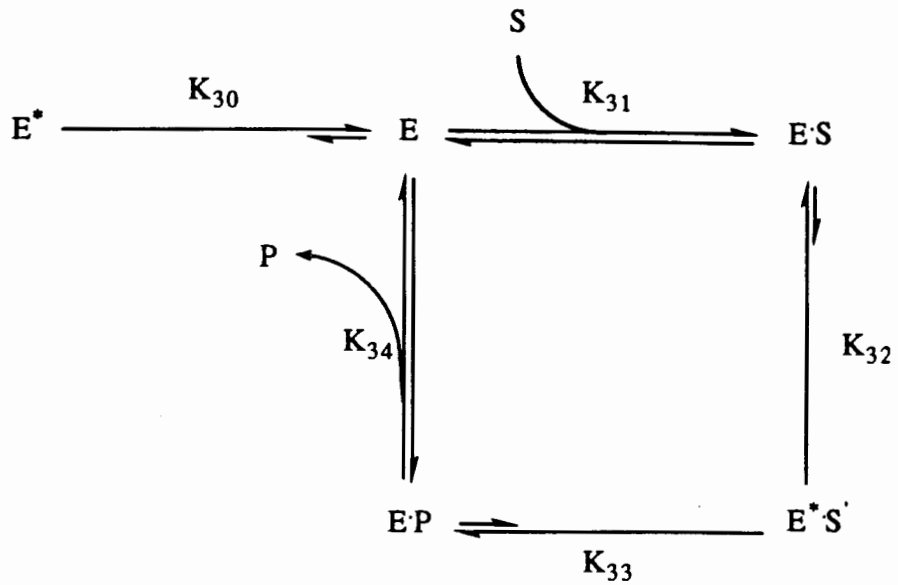

S = tetrahedral U-2',3'-P

S' = trigonal bipyramidal U-2',3'-P

E = inactive enzyme conformation

E^* = active enzyme conformation

P = U-3'-P (product)

(IV.3)

Schematic representation of the proposed mechanism of action of RNase A for the hydrolysis of U-2',3'-P

Although the pyrimidyl group is distant from the site of phosphate ester bond cleavage, it is suggested that binding of this group is important for the binding of the substrate to occur. Since it was shown that a pyrimidyl group is required for the whole inhibitor to be able to bind to the enzyme, it is suggested that the pyrimidyl group acts to induce a conformational change. This would result in a tight binding transition state complex. It must be understood that this complex is an analog of the actual transition state complex, therefore the hydrolysis of uridine 2',3'-cyclic monophosphate catalyzed by RNase A can be explained in the following way: When both the pyrimidyl and ribose-phosphate subsites of the active site are occupied, the enzyme brings the reactive groups together so that the full binding (optimum binding) of the highly unstable five-coordinate phosphate which is the transition state can be achieved (Fig. IV.2). Because the $E^*.S'$ transition state complex has a very high energy level, binding energy is required and this is provided by the pyrimidyl group so that the energy barrier to reach the transition state can be overcome. As can be seen, the tetrahedral substrate U-2',3'-P binds to the enzyme E, but the phosphate moiety is not in contact with the amino acid residues involved in catalysis (the K_m of U-2',3'-P and K_i of U are almost the same). Some support for this suggestion comes from the observation that the phosphate negative charge in a dinucleoside analog does not appear to directly contact either of the active-site histidine residues (50). When the transition

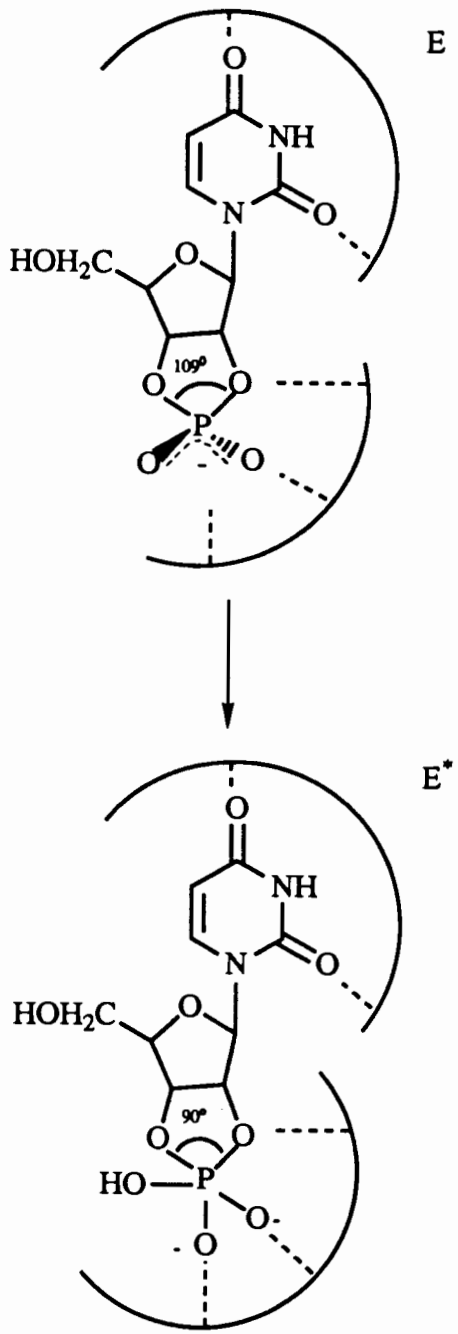

Fig. IV.2

Binding modes of the uridine 2',3'-cyclic monophosphate (substrate and transition state) to RNase A

state is reached, this phosphate becomes a pentacoordinate species which can make good contacts with these amino acid residues, resulting in catalysis by means of a transition-state stabilization. Direct evidence of transition-state stabilization in enzyme catalysis has been provided by the use of protein engineering on tyrosyl-tRNA synthetase (51).

Some evidence supporting that RNase A can exist in different conformations and that a conformational change is involved in the active site has been found. X-ray studies on the binding of cytidylic acid (2'-CMP) (52) and cytidine-N(3)-oxide 2' phosphate (O(3)-2'-CMP) (52,53) to RNase A have shown that their modes of binding are different and that they caused significant displacement of some side-chain atoms in the region of the active site, Lys-41 and His-119. Also, it was found that the location of Lys-7 and Lys-66 in the absence and presence of inhibitor at the active site was not the same (52,53). A mechanistic role for these lysine residues was suggested (53). Circular dichroism spectra of RNase A, free and complexed with competitive inhibitors (cytidine 2'-monophosphate and cytidine 3'-monophosphate), in the region 250 to 300 nm, have shown an environmental perturbation or conformational change resulting from the binding process (54). Even X-ray analysis has shown that the native or free enzyme exists in two different conformations, in which the imidazole ring of His-119 occupies two

different sites (A and B) (30). All this evidence supports the existence of at least two different conformations for RNase A.

Chapter V
Summary and Future Work

Vanadate complexes have been used previously to investigate the active site and mechanism of action of RNase A. In this work, vanadate complexed to ribose-containing ligands (uridine, 5,6-dihydrouridine and methyl β-D-ribofuranoside) resembling the reacting portion of uridine 2',3'-cyclic monophosphate, were used to study their interactions with RNase A. Neither vanadate alone nor vanadate complexed with methyl β-D-ribofuranoside were able to bind to RNase A. These results along with the absence of inhibition by the methyl β-D-ribofuranoside-vanadate complex shows that the pyrimidine group of the nucleotide which is the non-reacting portion of the substrate plays an important role in determining specificity. It is suggested that there is an interaction between the substrate and the enzyme mediated by the pyrimidine subsite, once it is occupied, that allows the tight binding of the transition state or transition state analog at the active site. It is also possible that once the pyrimidine group is bound, both the enzyme and the substrate undergo a small distortion or reorientation, since the C1'-N1 bond can rotate, so that the interaction between the catalytic groups in the enzyme and the substrate is optimum. The role of bound pyrimidine bases is also discussed based on X-ray refinement studies (53).

As postulated previously (9), the vanadate complexes studied that were able to bind to the enzyme, resembled the transition state more closely than the substrate uridine 2',3'-cyclic monophosphate. In the case of 2',3'-cyclic phosphates in solution, they adopt a tetrahedral geometry around the phosphorus atom, while for 2',3'-cyclic vanadates, besides the tetrahedral geometry, they also adopt a trigonal bipyramidal geometry around the vanadium atom, the transition state is shown (27,28) to have the latter geometry.

More work has to be done in order to obtain more qualitative and quantitative information about the active site and mechanism of action. X-ray crystallography cannot be obtained from substrate bound to active enzyme since digestion and diffusion take place in the crystal. However, neutron diffraction study on a uridine-vanadate complex (a transition state analog) bound to RNase A is available as well as NMR studies on His 12 and His 119, although these studies indicate that there is a direct interaction between His 119, the phosphate ion and Lys 41, it is difficult to accept that Lys 41 may act as a general acid-base catalyst at physiological pH.

^1H NMR spectroscopy may be useful in elucidating the role of His-12 and 119 and Lys-7, 41 and 66, in the mechanism of action of RNase A. PH studies are suggested, by using inhibitors which are substrate analogs and transition state analogs and observing their effects on the pK_a's of these amino acid residues.

Also, modifying the pyrimidine moiety of these inhibitors and studying their interactions with active site amino acid residues by NMR spectroscopy may be a useful approach to investigate the function of the pyrimidine binding subsite. Site directed mutagenesis on specific amino acid residues at the active site and NMR spectroscopy on this modified enzyme may be another useful approach.

References

(1) Chasteen, N. D. *Struct. Bonding* **1983**, *53*, 105-138.

(2) Gresser, M. J. and Tracey, A. S. *J. Am. Chem. Soc.* **1985**, *107*, 4215-4220.

(3) Gresser, M. J. and Tracey, A. S. *J. Am. Chem. Soc.* **1986**, *108*, 1935-1939.

(4) Tracey, A. S., Gresser, M. J. and Parkinson, K. M. *Inorg. Chem.* **1987**, *26*, 629-638.

(5) Tracey, A. S., Gresser, M. J. and Liu, S. *J. Am. Chem. Soc.* **1988**, *110*, 5869-5874.

(6) Robson. R. L., Eady, R. R., Richardson, T. H., Miller, R. W., Hawkins, M. and Postgate, J. R. *Nature* **1986**, *322*, 388-390.

(7) Boer, E. de, Kooyk, Y. van, Tromp, M. G. M., Plat, H. and Wever, R. *Biochim. Biophys. Acta* **1986**, *869*, 48-53.

(8) Rehder, D., Holst, H., Quaas, R., Hinrichs, W., Hahn, U. and Saenger, W. *J. Inorg. Biochem.* **1989**, *37*, 141-150.

(9) Lindquist, R. N., Lynn, J. L. Jr. and Lienhard, G. E. *J. Am. Chem. Soc.* **1973**, *95*, 8762-8768.

(10) Nour-Eldeen, A. F., Craig, M. M. and Gresser, M. J. *J. Biol. Chem.* **1985**, *260*, 6836-6842.

(11) Gresser, M. J. and Tracey, A. S. "Vanadium in Biochemical Systems" Klewer Academic Publishers.

(12) Craig, M. M., M. Sc. Thesis **1986**, Simon Fraser University.

(13) Drueckhammer, D. G., Durrwachter, J. R., Pederson, R. L., Crans, D. C., Daniels, L. and Wong, C. H. *J. Org. Chem.* **1988**, *51*, 70-77.

(14) Knowles, J. R. *Ann. Rev. Biochem.* **1980,** *49*, 877-919.

(15) Cotton, A. F. and Wilkinson, G. "Advanced Inorganic Chemistry" 3rd edition, Wiley Interscience **1972.**

(16) Percival, M. D., Doherty, K. and Gresser, M. J., unpublished results.

(17) Liu, S., M. Sc. Thesis **1989** Simon Fraser University.

(18) Berger. S. L. and Birkenmeier, C. S. *Biochemistry* **1979**, *18*, 5143-5149.

(19) Heyliger, C. E., Tahiliani, A. G. and McNeill, J. H. *Science* **1985**, *227*, 1474-1476.

(20) Tracey, A.S. and Gresser, M. J. *Proc. Natl. Acad. Sci.* **1986**, *83*, 609-613.

(21) Meyerovitch, J., Farfel, Z., Sack, J. and Shechter, Y. *J. Biol. Chem.* **1987**, *262*, 6658-6662.

(22) Ramanadham, S., Mongold, J. J., Brownsey, R. W., Cros, G. H. and McNeill, J. *Am. J. Physiol.* **1989**, *257*, H904-H911.

(23) Stankiewicz, P. J., Gresser, M. J., Tracey, A. S. and Hass, L. F. *Biochemistry* **1987**, *26*, 1264-1269.

(24) Richards, F. M. and Wyckoff, H. W. "Enzymes" 3rd edition **1971**, *4*, 647-806.

(25) Blackburn, P. and Moore, S. "The Enzymes" 3rd edition **1982**, *XV*, part B, 317-433.

(26) Wlodawer, A., Bott, R. and Sjolin, L. *J. Biol. Chem.* **1982**, *257*, 1325-1332.

(27) Wlodawer, A., Miller, M. and Sjolin, L. *Proc. Natl. Acad. Sci.* **1983**,*80*, 3628-3631.

(28) Borah, B., Chen, C., Egan, W., Miller, M., Wlodawer, A. and Cohen, J. S. *Biochemistry* **1985**, *24*, 2058-2067.

(29) Wyckoff, H. W., Tsernoglou, D., Hanson, A. W., Knox, J. R., Lee, B. and Richards, F. M. *J. Biol. Chem.* **1970**, *245*, 305-328.

(30) Borkakoti, N., Moss, D. S. and Palmer, R. A. *Acta Crystallogr.* **1982**, *B38*, 2210-2217.

(31) Sacharovsky, V. G., Chervin, I. I., Yakolev, G. I., Dudkin, S. M., Karpeisky, M. Ya., Shliapnikov, S. V. and Bystrov, V. F. *FEBS Lett.* **1973**, *33*, 323-326.

(32) Markley, J. L. *Biochemistry* **1975**, *14*, 3546-3553.

(33) Jentoft, J. E., Gerken, T. A., Jentoft, N. and Dearborn, D. G. *J. Biol. Chem.* **1981**, *256*, 231-236.

(34) Fersht, A. "Enzyme Structure and Mechanism" Freeman **1985**.

(35) Walsh, C. "Enzymatic Reaction Mechanisms" Freeman **1979**.

(36) Butler, A. and Danzitz, M. J. *J. Am. Chem. Soc.* **1987**, *109*, 1864-1865.

(37) Mason, J. "Multinuclear NMR" Plenum Press **1987**.

(38) Tracey, A. S. and Gresser, M. J. *Inorg. Chem.* **1988**, *27*, 1269-1275.

(39) Tracey, A. S. and Leon-Lai, C. H. *J. Am. Chem. Soc.* **1990**, submitted.

(40) Tracey, A. S., Jaswal, J., Gresser, M. J., Rehder, D. *Inorg. Chem.* **1990**, in press.

(41) Rao, C. N. R. "Ultraviolet and Visible Spectroscopy" 3rd edition **1975.**

(42) Motulsky, H. J. and Ransnas, L. A. *FASEB J.* **1987**, *1*, 365-374.

(43) Worthington Biochemical Corporation "Worthington Enzyme Manual" Freehold **1972.**

(44) Hummel, J. P. and Witzel, H. *J. Biol. Chem.* **1966**, *241*, 1023-1030.

(45) Del Rosario, E. J. and Hammes, G. G. *Biochemistry* **1969**, *8*, 1884-1889.

(46) Sawada, F. and Masachika, I. *J. Biochem.* **1969**, *66*, 415-418.

(47) Lienhard, G. E. *Science* **1973**, *180*, 149-154.

(48) Jencks, W. *Adv. Enzymol.* **1975**, *43*, 219-410.

(49) Koshland, D. E. *Adv. Enzymol.* **1960**, *22*, 45-97.

(50) Griffin, J. H., Schechter, A. N. and Cohen, J. S. *Ann. NY Acad. Sci.* **1973**, *222*, 693-708.

(51) Leatherbarrow, R. J., Fersht, A. R. and Winter, G. *Proc. Natl. Acad. Sci.* USA **1985**, *82*, 7840-7844.

(52) Howlin, B., Harris, G. W., Moss, D. S. and Palmer, R. A. *J. Mol. Biol.* **1987**, *196*, 159-164.

(53) Borkakoti, N. *Eur. J. Biochem.* **1983**, *132*, 89-94.

(54) Myer, Y. P., Barnard, E. A. and Pranab, K. P. *J. Biol. Chem.* **1979**, *254*, 137-142.